Variational boundary conditions for molecular dynamics simulations of crystalline solids at finite temperature: Treatment of the thermal bath

Xiantao Li
Department of Mathematics, Pennsylvania State University, University Park, Pennsylvania 16802, USA

Weinan E
Department of Mathematics and Program in Applied and Computational Mathematics, Princeton University, Princeton, New Jersey 08544, USA

(Received 9 March 2007; revised manuscript received 3 June 2007; published 18 September 2007)

This paper presents a systematic approach for finding efficient boundary conditions for molecular dynamics simulations of crystalline solids. These boundary conditions effectively eliminate phonon reflection at the boundary and at the same time allow the thermal energy from the bath to be introduced to the system. Our starting point is the Mori-Zwanzig formalism [R. Zwanzig, J. Chem. Phys. **32**, 1173 (1960); in *Systems Far from Equilibrium*, edited by L. Garrido (Interscience, New York, 1980); H. Mori, Prog. Theor. Phys. **33**, 423 (1965)] for eliminating the thermal bath, but we take the crucial next step that goes beyond this formalism in order to obtain memory kernels that decay faster. An equivalent variational formulation allows us to find the optimal approximate boundary conditions, after specifying the spatial-temporal domain of dependence for the positions of the boundary atoms. Application to a one-dimensional chain, a two-dimensional Lennard-Jones system, and a three-dimensional model of α-iron with embedded atom potential is presented to demonstrate the effectiveness of this approach.

DOI: 10.1103/PhysRevB.76.104107 PACS number(s): 31.15.Qg, 83.10.Mj, 61.43.Bn

I. INTRODUCTION

In this paper, we present a systematic treatment of the boundary conditions (BCs) for molecular dynamics (MD) simulations of crystalline solids at finite temperature. The present paper will focus only on the issue of handling the thermal bath. In subsequent papers, we will extend the framework presented here to the case when nontrivial external conditions, such as traction, are applied.[1] The issues discussed here not only are significant by themselves but also serve as a crucial step in developing multiscale modeling strategies that couple together atomistic and continuum models.[2–4]

Computer simulation based on MD has played an increasingly important role in studying the atomic structure and dynamic behavior of materials. A common problem in such a simulation is the effect of the boundaries: Due to its computational complexity, MD simulations are typically done on rather small systems which are truncated from much larger samples. As a result, artificial boundaries are introduced, where boundary conditions are needed to take into account the effect of the atoms that have been removed. Ideally, these boundary conditions should guarantee that the system behaves in the same way as if the whole sample is being simulated. In particular, such boundary conditions should have the following features.

(1) Allow the phonons generated from the simulation to propagate out, without being reflected.

(2) Be able to introduce thermal energy into the system as if the atoms that are removed from the simulation act as the thermal bath.

(3) Be able to handle external loading.

Much has been said about item (1) (see, in particular, Ref. 5). The present paper will be focused on item (2). In addition, we will present a general framework that allows us to discuss (1) and (2), and subsequently (3) in a unified fashion.

The setup is illustrated in Fig. 1. The computational domain, denoted by D, consists of atoms that are represented by the filled circles. The entire sample is denoted by Ω which also contains atoms, represented by open circles, that will be removed from the simulation. We will call the removed atoms the bath atoms. We start with molecular dynamics for the entire system,

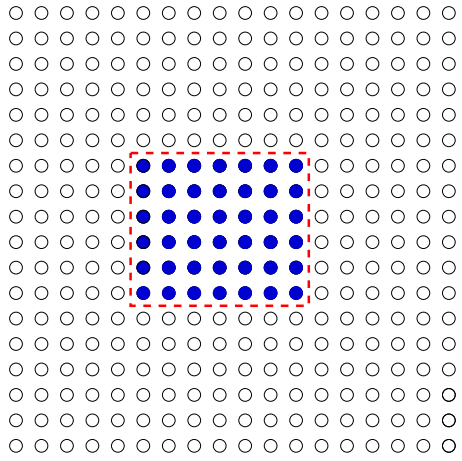

FIG. 1. (Color online) A schematic of the setup of the problem. Filled circles: Atoms in the computational domain. Open circles: Atoms in the heat bath. The dashed line indicates the interface between the two groups and defines the boundary for the computational domain.

$$m\ddot{\mathbf{u}}_i = -\nabla_{\mathbf{u}_i}\Phi, \quad i \in \Omega,$$

where m is the mass, $\mathbf{u}_i$ is the displacement of the ith atom, and Φ is the potential energy of the system. The main assumptions are as follows.

(1) Bath atoms are in thermal equilibrium initially.

(2) The interaction among bath atoms and the interaction between bath atoms with the atoms in D are linear.

There is no restriction on the interaction between the atoms in D. These assumptions are fine in the absence of plastic deformation. However, they are violated when dislocations or other plastic defects move across the boundary of D. This is the major shortcoming of the present approach.

In principle, the Mori-Zwanzig formalism[6–9] provides an ideal framework for eliminating the bath atoms. A typical result from such a reduction procedure is the generalized Langevin equation (GLE) for the remaining atoms, $i \in D$, in the form of

$$m\ddot{\mathbf{u}}_i = -\nabla_{\mathbf{u}_i}V + D_i\mathbf{u}_i + \sum_{j\in D}\left[\boldsymbol{\theta}_{ij}(0)\mathbf{u}_j(t) - \int_0^t \boldsymbol{\theta}_{ij}(t-s)\dot{\mathbf{u}}_j(s)ds\right] + F_i(t). \tag{1}$$

Here, D_i is a constant matrix and V is the potential energy for the subset D. The functions $\boldsymbol{\theta}_{ij}(t)$, known as the *memory kernels*, describe the history dependence of the process after the bath atoms are eliminated. $F_i(t)$, which can be considered as random forcing, is related to the dynamics of the unresolved bath atoms. In the context of molecular dynamics, the GLE approach was first used by Adelman and Doll in[10,11] to study gas-surface interaction, where a one-dimensional chain model was considered to model the atoms in the solid. This formulation was later extended to body-centered and face-centered cubic crystal lattices by Tully.[12] Recently, Cai *et al.*[13] discussed how one can obtain such exact kernels in the general case by performing a large number of test simulations. Berne and co-workers[14,15] and Izvekov and Voth[16] considered this problem for liquids and used MD simulations to extract the memory kernels. Karpov, Liu, Wagner and co-workers continued with this path and extended the formalism to general crystal structures.[17–19]

However, as is usually the case with the Mori-Zwanzig formalism, even though it is in principle exact, it is difficult to use in practice. For the present problem, this difficulty is reflected in the slow decay and long interaction range of the memory kernels which couple together all the boundary atoms and their time history. This is a rather substantial computational overhead. In addition, if for any reason we would like to move the computational domain during the simulation, for example, to track the path of a defect, we run into difficulties with the fact that the previous history of the new boundary atoms is not available. This is a serious problem if we want to couple MD simulations with continuum modeling in a multiscale, multiphysics setting.

Therefore, the central issue is to find approximate boundary conditions that allow us to represent the effect of the bath atoms with reasonable accuracy and complexity. In the general context, the need to approximate the Mori-Zwanzig formalism has been recognized by Chorin *et al.* in their work on optimal prediction.[20–23] In the present context, this idea was first pursued in the work of E and Huang[2,3] for simplified models, and later for general crystal structure by Li and E.[5] This series of work is limited to zero temperature in which case the main requirement for the boundary conditions is to prevent the reflection of the phonons. These local boundary conditions, which are obtained from a variational formulation that aims at minimizing phonon reflection, are referred to as variational boundary conditions (VBCs).

The present paper extends this series of work to finite temperature. At finite temperature, the issue is not simply phonon reflection, but also the absorption of phonon energy from the environment. Our philosophy is very much in line with that of optimal prediction: Given the allowed complexity of the boundary condition, in the form of the set of neighboring atoms that a boundary atom is allowed to interact with and the duration of the time history that the boundary atoms depend on, we would like to find the optimal interaction kernels—in the sense that the reflection of outward propagating phonons is minimized. It is not yet clear how to find variational approximations of the Mori-Zwanzig formalism in the general setting. Our work is possible because of the following special features of the problem.

(1) The memory kernels are independent of temperature.

(2) The exact memory kernels can be characterized by a variational principle.

(3) The memory kernels are not unique. More efficient memory kernels can be found by "trading spatial dependence for temporal dependence," namely, by increasing their spatial interaction range, we can obtain memory kernels that decay faster in time.

In implementing such a program, there are several numerical issues that have to be addressed, such as the stability of the algorithm, efficient procedures for sampling the noise, and error control. We will discuss these issues in detail. We will continue to call the boundary conditions developed here VBCs.

The first application of such boundary conditions is that they can be used as thermostats. In fact, since they come from explicit representation of the effect of the bath atoms, one expects them to perform well as thermostats. We will present examples demonstrating that this is indeed the case. Compared with the commonly used thermostats, the current method has the feature that it controls the system temperature from the boundary without directly affecting the dynamics in the interior. This is particularly attractive when simulating the dynamics of inhomogeneous system, e.g., systems that contain material defects. However, even for homogeneous systems it has been a concern whether existing thermostating techniques, such as Andersen's thermostat,[24] the isokinetic method,[25] and Berendsen's method,[26] give the correct dynamic behavior (see the discussion in Ref. 27). For this reason, we will show comparisons between the measured velocity correlation functions using VBC and the exact ones. More sophisticated examples will be presented in subsequent publications after we discuss how to handle external deformation or loading.

Another approach for prescribing the boundary condition is to replace the atoms in the heat bath with a coarser model.

This idea has been pursued by Rudd and Broughton[28] in their work on coarse-grained molecular dynamics (CGMD). Similar to the Mori-Zwanzig procedure, the main idea in CGMD is to integrate out the excess atomic degrees of freedom in the heat bath and obtain a reduced dynamic model for the displacement field represented by finite elements. CGMD makes the strong assumption that the eliminated degrees of freedom are close to thermal equilibrium with the coarse-grained variable. In contrast, the procedure presented here can, in principle, be made as accurate as we wish.

In order to deal with much larger systems, we will have to consider the problem in a multiscale setting. This brings out many interesting issues, such as the ghost forces, stress and energy calculation in the continuum region, statistical error, etc. They will be addressed in separate work along with further comparison with the CGMD method.

II. MORI-ZWANZIG FORMALISM

A. Quick review

The basic setup of the problem is shown in Fig. 1. We divide the atoms in a crystalline solid into two groups: One group consists of atoms that we will keep in our computational domain. The variables associated with these atoms are called the *retained variables*. The rest are treated as the heat bath and the variables associated with them will be eliminated from the formulation. The purpose of the heat bath is twofold: First, it provides the phonons that maintain the whole system at certain temperature. Second, it helps absorb the phonons and elastic waves that are generated from the computational domain.

Our purpose is to eliminate the atoms that are outside the computational domain. For this purpose, we adopt the Mori-Zwanzig formalism, which is a general procedure for eliminating variables in a system. The effects of the eliminated degrees of freedom are represented in memory kernels and noise terms for the dynamics of the retained variables.

To briefly illustrate the ideas, let us recall the model problem introduced in Ref. 29. The system of interest has one degree of freedom, which is coupled with many other degrees of freedom that act as the heat bath. These are modeled by independent harmonic oscillators. A similar model with coupled oscillators was considered in Ref. 30. The Hamiltonian for the entire system is written as

$$H = \frac{1}{2}v^2 + U(x) + \sum_{j=1}^{N}\left[\frac{1}{2}p_j^2 + \frac{1}{2}\omega_j^2\left(q_j - \frac{\gamma_j}{\omega_j^2}x\right)^2\right].$$

Here, the masses of all the particles are assumed to be unity. ω_j is the frequency of the jth oscillator and γ_j is the coupling constant. Hamilton's equations read

$$\dot{x} = v,$$

$$\dot{v} = -U'(x) + \sum_j \gamma_j\left(q_j - \frac{\gamma_j}{\omega_j^2}x\right),$$

$$\dot{q}_j = p_j,$$

$$\dot{p}_j = -\omega_j^2 q_j + \gamma_j x.$$

The last two equations above can be solved analytically, yielding

$$q_j(t) = \frac{\gamma_j}{\omega_j^2}x(t) + \left[q_j(0) - \frac{\gamma_j}{\omega_j^2}x(0)\right]\cos\omega_j t + \frac{p_j(0)}{\omega_j}\sin\omega_j t - \frac{\gamma_j}{\omega_j^2}\int_0^t \cos\omega_j(t-s)v(s)ds.$$

Substituting this into the second equation gives

$$\dot{v} = -U'(x) - \int_0^t K(t-s)v(s)ds + F(t), \tag{2}$$

where

$$K(t) = \sum_j \frac{\gamma_j^2}{\omega_j^2}\cos\omega_j t$$

and

$$F(t) = \sum_j \gamma_j\left[q_j(0) - \frac{\gamma_j}{\omega_j^2}x(0)\right]\cos\omega_j t + \frac{\gamma_j}{\omega_j}p_j(0)\sin\omega_j t.$$

Equations in the form of Eq. (2) are known as the GLEs. The first term on the right hand side describes the interaction among the retained variables. The second term describes history dependence of the dynamics: After eliminating the degrees of freedom associated with the heat bath, the dynamics is no longer Markovian. The last term, which represents the influence of the heat bath, is often regarded as the random force. We will assume that for any initial value of x, the initial configuration of the heat bath obeys the canonical distribution,

$$\rho(q_1,p_1,\ldots,q_N,p_N) = \frac{1}{Z}e^{-\beta H}, \tag{3}$$

with temperature $T=1/(k_B\beta)$. It is easy to see that $F(t)$ is a Gaussian process with mean zero and covariance

$$\langle F(t+t_0)F(t_0)\rangle = k_B T\sum_j \frac{\gamma_j^2}{\omega_j^2}\cos\omega_j t = k_B T K(t).$$

In particular, the process is stationary. More importantly, the time correlation of the random noise is related to the memory kernel in the GLE. This is the essence of the fluctuation-dissipation theorem.[8]

In the general case, it is more convenient to use the projection operator formalism.[6,8,20–23] Following Chorin *et al.*, we will view the projection as conditional expectation. Consider a system of ordinary differential equations for the variables $\mathbf{x}=(x_1,x_2,\ldots,x_n)$,

$$\frac{d}{dt}\mathbf{x}(t) = \mathbf{f}(\mathbf{x}(t)), \quad \mathbf{x}(0) = \mathbf{x}^0. \tag{4}$$

Assume that the first m degrees of freedom are to be kept (retained variables). The rest will be eliminated. For any function $g(\mathbf{x})$, define the projection of g by

$$Pg = \mathbf{E}(g|x_1, x_2, \ldots, x_m) = \frac{\int g(\mathbf{x})\rho(\mathbf{x})dx_{m+1}\cdots dx_n}{\int \rho(\mathbf{x})dx_{m+1}\cdots dx_n},$$

where ρ is a probability density, often taken to be the equilibrium distribution for the system (4).

Consider the Liouville equation

$$\frac{d}{dt}u(\mathbf{x},t) = Lu(\mathbf{x},t), \tag{5}$$

where L is the Liouville operator,

$$L = \sum_i f_i(\mathbf{x})\partial_{x_i}. \tag{6}$$

The solution $u(\mathbf{x},t)$ of Eq. (5) can be expressed as

$$u(\mathbf{x},t) = e^{tL}u(\mathbf{x},0). \tag{7}$$

Let $\varphi(t)=\varphi(\mathbf{x}(t))$ be any function of the retained variables at time t, with initial condition $\varphi(0)$. With the semigroup notation in Eq. (7), this can be written as $\varphi(t)=e^{tL}\varphi(0)$. The goal of the projection procedure is to derive an effective equation for $\varphi(t)$. Taking the time derivative, we have

$$\frac{d}{dt}\varphi(t) = e^{tL}L\varphi(0) = e^{tL}PL\varphi(0) + e^{tL}QL\varphi(0),$$

where $Q=I-P$. Next, using Dyson's formula,

$$e^{tL} = e^{tQL} + \int_0^t e^{(t-s)L}PLe^{sQL}ds,$$

the second term can be written as

$$e^{tL}QL\varphi(0) = e^{tQL}QL\varphi(0) + \int_0^t e^{(t-s)L}PLe^{sQL}QL\varphi(0)ds.$$

Defining

$$F(t) = e^{tQL}QL\varphi(0), \quad K(t) = PLF(t)$$

and combining all the terms, we get

$$\frac{d}{dt}\varphi(t) = e^{tL}PL\varphi(0) + \int_0^t e^{(t-s)L}K(s)ds + F(t). \tag{8}$$

The first and second terms on the right hand side depend only on the retained variables. They represent, respectively, the Markovian contribution and the history dependence of the dynamics for the retained variables. The third term, which satisfies $PF=0$, depends on the initial condition of the heat bath variables. Since the statistics of the heat bath is assumed, $F(t)$ can be regarded as random noise.

B. Application to molecular dynamics modeling of solids

Now, we turn our attention to the case of molecular dynamics for solids. Let $\mathbf{r}_i$ and $\mathbf{x}_i$ be the equilibrium and current position of the ith atom, respectively, and let $\mathbf{u}_i=\mathbf{x}_i-\mathbf{r}_i$ be the displacement vector. Alternatively, we will use $\mathbf{u}(\mathbf{r}_i,t)$ to represent the displacement of the ith atom whenever it is more convenient. For simplicity, we assume that the boundary is planar with inward normal vector $\mathbf{n}$, and we assume that the retained variables are the ones associated with the atoms that satisfy $\mathbf{r}_i\cdot\mathbf{n}>0$, namely, all the atoms on the right, and we let $\hat{\mathbf{u}}=\{\mathbf{u}_i:\mathbf{r}_i\cdot\mathbf{n}>0\}$.

The dynamics of the atoms is described by Newton's equation,

$$m\ddot{\mathbf{u}}_i = -\nabla_{\mathbf{u}_i}\Phi, \tag{9}$$

with atomic potential Φ. In accordance with the projection procedure, we choose the variables $\mathbf{x}$ in Eq. (4) to be the displacement and momenta of all the atoms,

$$\mathbf{x} = (\mathbf{u}_1, m\mathbf{v}_1, \ldots, \mathbf{u}_n, m\mathbf{v}_n).$$

The Liouville operator in this case becomes

$$L = \sum_i \mathbf{v}_i\cdot\nabla_{\mathbf{u}_i} - \nabla_{\mathbf{u}_i}H/m\cdot\nabla_{\mathbf{v}_i}.$$

To proceed further, we make a harmonic approximation for the interaction with the bath atoms. For the retained variables, we keep the original nonlinear potential, denoted by $V(\hat{\mathbf{u}})$. The Hamiltonian for the entire system can be written as

$$H = \frac{1}{2}\sum_i m\mathbf{v}_i^2 + V(\hat{\mathbf{u}}) + \frac{1}{2}\sum_{\mathbf{r}_i\cdot\mathbf{n}\leq 0}\sum_k \mathbf{u}_i^T D_k \mathbf{u}_{i+k}. \tag{10}$$

Here, D_k is the force constant for the harmonic approximation. The third term in the equation implies that the atomic interaction involving the atoms in the bath is linear. Following the Mori-Zwanzig procedure, we obtain the following GLE for the retained variables:

$$m\ddot{\mathbf{u}}_i = -\nabla_{\mathbf{u}_i}V - \left(\sum_{\substack{k\in K\\ \mathbf{r}_{i-k}\cdot\mathbf{n}\leq 0}} D_{-k}\right)\mathbf{u}_i + \sum_{\mathbf{r}_j\cdot\mathbf{n}>0}\left[\boldsymbol{\theta}_{i,j}(0)\mathbf{u}_j - \int_0^t \boldsymbol{\theta}_{i,j}(s)\dot{\mathbf{u}}_j(t-s)ds\right] + F_i(t). \tag{11}$$

Provided that the initial data for the bath variables are drawn from the Gibbs distribution, the random processes $F_i(t)$ are stationary Gaussian processes. In addition, the fluctuation-dissipation theorem holds

$$\langle F_i(t)F_j(0)^T\rangle = k_BT\boldsymbol{\theta}_{i,j}(t). \tag{12}$$

See Appendix A for the detailed calculations.

For atomic potentials of finite range, the memory and the random noise terms are localized to those atoms that have direct interaction with the heat bath. In fact, for atoms inside the computational domain that satisfy $\mathbf{r}_i\cdot\mathbf{n}>r_c$, i.e., the distance to the boundary is larger than the cut-off radius, we have $QL\mathbf{v}_i(0)=0$. Hence, both the random noise and memory term vanish from the GLEs (11). This is demonstrated in Fig. 2, where a triangular lattice is plotted with different orientations. Here, nearest neighbor interactions are assumed. In Fig. 2(a), the normal vector is (0, 1) and there is only one

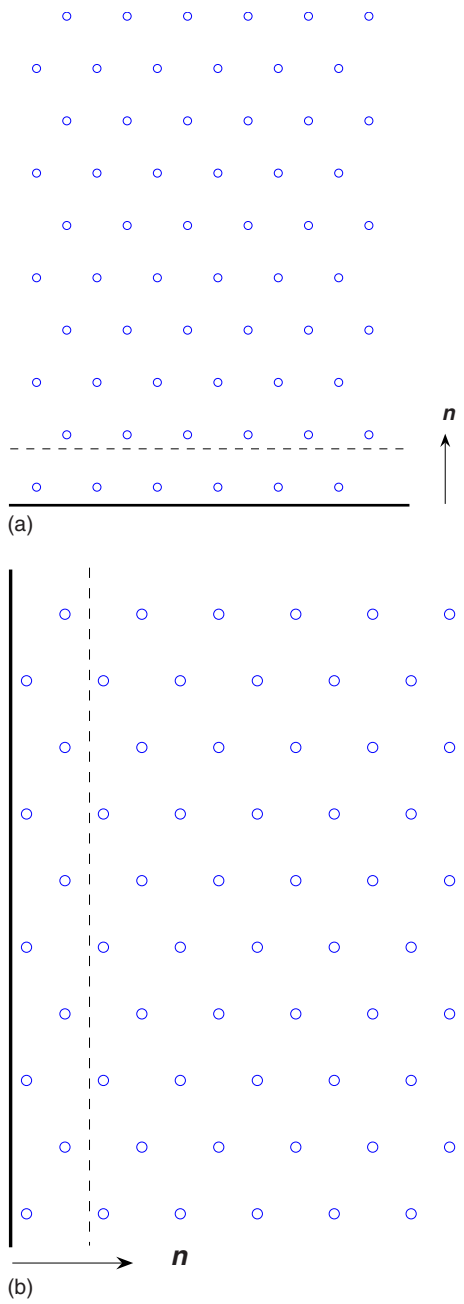

FIG. 2. (Color online) Boundary condition for molecular dynamics simulation of a two-dimensional triangular lattice. (a) $\mathbf{n}=(1,0)$. In this case, there is only one layer of atoms on which the random forces need to be introduced, i.e., $F_i \neq 0$. (b) $\mathbf{n}=(0,1)$. In this case, there are two layers of such atoms.

layer on which the memory and the random force terms need to be added, whereas in Fig. 2(b) the normal vector is (0, 1) and there are two such layers because the cut-off radius spreads over two atomic spacings. However, we can include two successive atoms in a single unit cell and view the system as a "complex lattice." The force constant and the atomic mass will also be redefined accordingly. As a result, we can rewrite the equation of motion in terms of the extended variables and always assume, without loss of generality, that in the normal direction the atomic interaction is only with the nearest neighbors. We define

$$J_0 = \{j:\mathbf{r}_j \cdot \mathbf{n} = 0\}, \tag{13}$$

which represents the layer of atoms in the heat bath that are adjacent to the boundary, and

$$J_1 = \{j:\mathbf{r}_j \cdot \mathbf{n} = d_n\}, \tag{14}$$

which represents the atoms at the boundary with d_n being the atomic spacing along the normal direction. Now, we can simplify the GLE (11) to

$$m\ddot{\mathbf{u}}_i = -\nabla_{\mathbf{u}_i} V - \left(\sum_{k\in J_1} D_{-k}\right)\mathbf{u}_i + \sum_{j\in J_1}\left[\boldsymbol{\theta}_{i-j}(0)\mathbf{u}_j(t) - \int_0^t \boldsymbol{\theta}_{i-j}(s)\dot{\mathbf{u}}_j(t-s)ds\right] + F_i(t) \tag{15}$$

for all $i \in J_1$, and the fluctuation-dissipation theorem becomes

$$\langle F_i(t)F_j(0)^T\rangle = k_B T\boldsymbol{\theta}_{i-j}(t). \tag{16}$$

The size of the vectors $\mathbf{u}_i$ and F_i is $d\times n_a$, with n_a the number of atoms in each unit cell. Another result from our calculation is that at zero temperature the GLEs (15) are equivalent to the following boundary condition for any atom i, $i \in J_0$:

$$\mathbf{u}(\mathbf{r}_i,t) = \sum_{j\in J_1}\int_0^t \boldsymbol{\alpha}_j(s)\mathbf{u}(\mathbf{r}_{i+j},t-s)ds. \tag{17}$$

This suggests that the displacement for the atoms at the boundary can be expressed in terms of the displacement of the atoms in the interior.

C. Example

To illustrate the Mori-Zwanzig procedure, we consider the simplest example—a one-dimensional chain of atoms with nearest neighbor interaction

$$m\ddot{x}_j = \varphi'(x_{j+1}-x_j) - \varphi'(x_j - x_{j-1}), \tag{18}$$

via the Lennard-Jones potential

$$\phi(r) = 4\epsilon[(\sigma/r)^{12} - (\sigma/r)^6]. \tag{19}$$

The lattice parameter for this system is $a_0 = \sqrt[6]{2}\sigma$, and the displacement is defined as $u_j = x_j - ja_0$.

The phonon dispersion relation for this system is given by

$$\omega(k)^2 = \frac{K^2}{m}[2-2\cos(ka_0)], \quad k \in \left[-\frac{\pi}{a_0},\frac{\pi}{a_0}\right], \tag{20}$$

where

$$K^2 = \phi''(a_0).$$

We define the heat bath as the set of atoms with $j \leqslant 0$. After adopting the harmonic approximation for the heat bath atoms, we obtain the following Hamiltonian for the whole system:

$$H = \sum_{j\leqslant 0} \frac{K^2}{2}(u_{j+1}-u_j)^2 + \sum_{j>0} \phi(x_{j+1}-x_j) + \sum_j \frac{1}{2}mv_j^2.$$

The projection procedure gives rise to GLEs of the form

$$\begin{aligned} m\ddot{u}_1 &= \phi'(x_2-x_1) - \int_0^t \theta(t-s)\dot{u}_1(s)ds + F(t), \\ m\ddot{u}_j &= \phi'(x_{j+1}-x_j) - \phi'(x_j-x_{j-1}), \quad j>1. \end{aligned} \tag{21}$$

The GLE for the first atom is equivalent to the following boundary condition:

$$u_0 = u_1(0)\int_t^\infty \alpha(s)ds + \int_0^t \alpha(s)u_1(t-s)ds + F(t),$$

where

$$\int_t^\infty \alpha(s)ds = \theta(t).$$

As will be shown in Eq. (A10) in Appendix A, the random process $F(t)$ can be written as

$$F(t) = \sum_{j\leqslant 0} c_j(t)[u_{j+1}(0)-u_j(0)] + s_j(t)v_j(0).$$

The coefficients $c_j(t)$ and $s_j(t)$ are governed by

$$\dot{s}_j = c_{j-1} - c_j,$$

$$m\dot{c}_j = K^2(s_j - s_{j+1}),$$

$$s_0(t) = 0, \quad s_j(0) = 0, \quad c_j(0) = -K^2\delta_{j+1}, \quad j\leqslant 0,$$

from which we find

$$s_{-1}(t) = -\frac{2K^2}{\pi}\int_0^\pi \frac{\sin^2 k \sin \omega t}{\omega}dk$$

and

$$\theta(t) = -c_{-1}(t) = \frac{K^2}{\pi}\int_0^\pi \frac{\sin^2 k \cos \omega t}{1-\cos k}dk.$$

Taking the Laplace transform, we get

$$\hat{\theta}(s) = \frac{m}{2}\sqrt{s^2 + 4K^2/m} - \frac{m}{2}s.$$

Thus, we have

$$\theta(t) = \frac{\sqrt{m}K}{t}J_1\left(\frac{2Kt}{\sqrt{m}}\right) \tag{22}$$

and

$$\alpha(t) = \frac{2}{t}J_2\left(\frac{2Kt}{\sqrt{m}}\right), \tag{23}$$

where J_1 and J_2 are the Bessel functions of the first kind.

Lastly, the random process $F(t)$ is a stationary Gaussian process with time correlation,

$$\langle F(t)F(0)\rangle = k_B T\theta(t).$$

For this one-dimensional model, the GLE in the same form was derived by Adelman and Doll[10,11] using a different procedure.

III. GENERALIZED LANGEVIN EQUATION AND PHONON REFLECTION

In principle, Eqs. (11) and (A16) derived from Mori-Zwanzig procedure give us the exact boundary condition after eliminating the heat bath variables, provided that the dynamics of the bath atoms is accurately approximated by the linear models. However, in the present form the GLEs are difficult for practical use due to the long range interaction in the memory kernels. To find efficient and accurate approximations of the GLE, we will need an alternative description of these memory kernels.

Observe that since the memory kernels are independent of the temperature, we can restrict our attention to the case of zero temperature, in which case the boundary condition should allow the phonons to propagate out without being reflected at the boundary. The purpose of this section is to show that the GLE (11) is, in fact, equivalent to nonreflecting boundary conditions at zero temperature.

A. Reflection matrices

Since phonon reflection is a basic concern, we will briefly review the key relevant concepts. We adopt a harmonic approximation of the interatomic potential,

$$\Phi(\mathbf{u}_1, \mathbf{u}_2, \ldots, \mathbf{u}_n) = \Phi_0 + \frac{1}{2}\sum_{i\neq j} \mathbf{u}_i^T D_{i-j}\mathbf{u}_j. \tag{24}$$

The Fourier transform of the force constants defines the dynamic matrix

$$\mathcal{D}(\mathbf{k}) = \sum_j D_j e^{-i\mathbf{k}\cdot\mathbf{r}_j}. \tag{25}$$

The dispersion relation of this system is related to the eigenvalues λ_s of the matrix $\mathcal{D}$ by

$$\omega_s^2 = \lambda_s.$$

For definiteness, we will take $\omega_s = \sqrt{\lambda_s}$. The corresponding eigenvectors $\boldsymbol{\varepsilon}_s(\mathbf{k})$ are the polarization vectors. We will use the standard normalization

$$\boldsymbol{\varepsilon}_s \cdot \boldsymbol{\varepsilon}_{s'} = \delta_{ss'}.$$

The index $1\leqslant s\leqslant S$ designates the different phonon branches and S is the number of branches in the spectrum. A phonon mode is represented by a wave number $\mathbf{k}$ restricted to the first Brillouin zone B.

Next, we define the reflection matrices for the phonons. The reflected phonon modes are determined by the conditions that the displacement and strain are continuous before and after phonon reflection. This implies that the frequency and the tangential component of the wave number should be conserved. To be more specific, let $\mathbf{k}^I$ and $\mathbf{k}^R$ be the wave

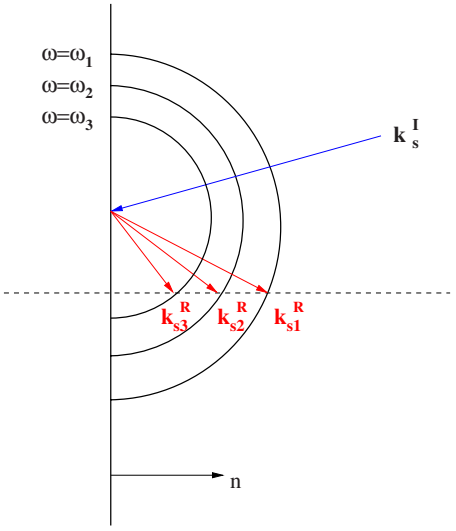

FIG. 3. (Color online) A schematic of the phonon reflection at the boundary. The vertical line shows the boundary with normal direction $\mathbf{n}$. An incident wave from branch s with wave number $\mathbf{k}_s^I$ and frequency ω arrives at the boundary, generating three reflected waves with wave number $\mathbf{k}_{ss'}^R$. The second subscript s', $1 \leqslant s' \leqslant 3$, represents the branches that the reflected waves belong to. The frequency of the reflected waves must match that of the incident wave. Therefore, these wave numbers should be in the level sets $\omega_{s'}(\mathbf{k}) = \omega$, as indicated by the curves in the picture, where $\omega_{s'}$ is the dispersion relation for the s' branch. In addition, their tangential components have to be equal from Eq. (26). The horizontal dashed line in this figure is a plane that contains all such wave numbers. Therefore, the intersection of the level sets and the horizontal plane determines the wave numbers $\mathbf{k}_{ss'}^R$.

numbers corresponding to the incident and reflected phonon mode respectively, and $\mathbf{k}^I \in B$. Then, $\mathbf{k}^R$ must satisfy

$$\mathbf{k}^I - (\mathbf{k}^I \cdot \mathbf{n})\mathbf{n} = \mathbf{k}^R - (\mathbf{k}^R \cdot \mathbf{n})\mathbf{n}, \quad \omega_s(\mathbf{k}) = \omega_{s'}(\mathbf{k}^R), \quad (26)$$

for some $1 \leqslant s, s' \leqslant S$.

Solving these equations can be quite complicated. We have found an alternative procedure, in which the problem of finding the reflected wave mode was reduced to finding the zeros of a polynomial.[5] The degree of the polynomial depends on S and on the effective range of the interatomic potential, denoted by N_e, which is the number of layers along the normal direction that have direct interaction with the boundary atoms. We will denote the reflected phonon mode by

$$\{\mathbf{k}_{ss'}^R, s' = 1,2, \ldots, N_R\}, \quad N_R = SN_e.$$

The boundary reflection is demonstrated in Fig. 3. With the assumption that we made in the previous section, $N_e = 1$. Hence, $N_R = S$.

To compute the reflection coefficients, consider a superposition of an incident wave on the branch s and the resulting reflected waves,

$$\mathbf{u}_j(t) = e^{i(\mathbf{k}\cdot\mathbf{r}_j - \omega_s t)}\boldsymbol{\varepsilon}_s(\mathbf{k}) + \sum_{s'} R_{ss'} e^{i(\mathbf{k}_{ss'}^R \cdot \mathbf{r}_j - \omega_s t)}\boldsymbol{\varepsilon}_{s'}(\mathbf{k}_{ss'}^R). \quad (27)$$

We will restrict our attention to boundary conditions in the form of Eq. (17). A substitution into Eq. (17), or equivalently, to the GLE (15), leads to a linear system, from which the reflection coefficients $R_{ss'}(\mathbf{k})$ can be obtained. Recall that from Eq. (13), $J_0 = \{\mathbf{r}_j : \mathbf{r}_j \cdot \mathbf{n} = 0\}$ contains the heat bath atoms next to the boundary, and for the atoms at the boundary, $J_1 = \{\mathbf{r}_j : \mathbf{r}_j \cdot \mathbf{n} = d_n\}$, with d_n the lattice spacing in the normal direction. For any $\mathbf{k} \in B$, define

$$A(\mathbf{k}) = \sum_j \int_0^{+\infty} \boldsymbol{\alpha}_j(\tau) e^{-i(\mathbf{k}\cdot\mathbf{r}_j + \omega\tau)} d\tau, \quad (28)$$

which corresponds to a discrete Fourier transform along the boundary and a Fourier/Laplace transform in time. A direct substitution of Eq. (27) into Eq. (17) leads to

$$(I - e^{id_n k^n}\bar{A})\boldsymbol{\varepsilon}_s + \sum_{s'} R_{ss'}(\mathbf{k})(I - e^{id_n k_{ss'}^n}\bar{A})\boldsymbol{\varepsilon}_{s'}(\mathbf{k}_{ss'}^R) = 0, \quad (29)$$

where the bar denotes the complex conjugate. These equations form a linear system from which the reflection coefficients R can be computed.

The exact boundary condition or memory kernel is obtained by requiring that the reflection coefficient vanish identically. For the one-dimensional example discussed earlier, if we consider boundary conditions of the form

$$u_{-1}(t) = \int_0^t \alpha(s) u_0(t-s) ds, \quad (30)$$

the reflection coefficients $R(k)$ can be expressed as (see also Refs. 2 and 3)

$$R(k) = -\frac{1 - \hat{\alpha}(\omega)e^{ika_0}}{1 - \hat{\alpha}(\omega)e^{-ika_0}}, \quad k \in \left(-\frac{\pi}{a_0}, 0\right). \quad (31)$$

Here, $\hat{\alpha}(\omega)$ is the Fourier/Laplace transform of $\alpha(t)$,

$$\hat{\alpha}(\omega) = \int_0^{\infty} \alpha(t) e^{-i\omega t} dt. \quad (32)$$

k and ω are related by the dispersion relation (20).

B. Equivalence of the generalized Langevin equation with nonreflecting boundary conditions

Here, we provide an equivalent characterization of the memory kernels using the reflection matrices. We will prove the following statement: The memory kernels are exact if the corresponding reflection coefficients are zero for all wave numbers.

The proof is as follows. First, we obtain the exact boundary condition (17) via Fourier and Laplace transforms in the case of zero temperature. Then, we check the reflection coefficient using Eq. (29). At zero temperature, the initial con-

dition for the heat bath variables is zero. Namely,

$$\mathbf{u}_j(0)=0, \quad \dot{\mathbf{u}}_j(0)=0,$$

for all $\mathbf{r}_j\cdot\mathbf{n}\leqslant 0$.

In this case, the solution for the atoms in the heat bath can be expressed analytically. We first take a Fourier transform of the displacement along planes tangent to the boundary,

$$U_m(\mathbf{k},t)=\mathcal{F}_{j\to\mathbf{k}}\mathbf{u}_j=\sum_{\mathbf{r}_j\cdot\mathbf{n}=md_n}\mathbf{u}_j e^{-\mathbf{k}\cdot\mathbf{r}_j},$$

for $\mathbf{k}\cdot\mathbf{n}=0$. Then, Newton's equations (9) become

$$M\ddot{U}_m=\hat{D}_{-1}U_{m-1}+\hat{D}_0U_m+\hat{D}_1U_{m+1},$$

with $U_1(t)$ given. M is the mass matrix. Note that we have used the assumption that the atomic interaction is only via nearest neighbors in the normal direction.

Next, we take a Laplace transform in time,

$$\tilde{U}_m(\mathbf{k},s)=\mathcal{L}_{t\to s}\{U_m(\mathbf{k},t)\},$$

which leads to a set of difference equations,

$$s^2M\tilde{U}_m=\hat{D}_{-1}\tilde{U}_{m-1}+\hat{D}_0\tilde{U}_m+\hat{D}_1\tilde{U}_{m+1}. \tag{33}$$

Let the eigenvalues and eigenvectors of the difference equations be λ_l and $\boldsymbol{\epsilon}_l$, respectively. We can then write the general solution of Eq. (33) as

$$\tilde{U}_m(\mathbf{k},s)=\sum_{|\lambda_l|>1}c_l\lambda_l^m\boldsymbol{\epsilon}_l, \tag{34}$$

with constant c_l. Here, we have excluded the mode for which $|\lambda_l|<1$ to guarantee that the solution is bounded. In particular, we have

$$\tilde{U}_0=E\Lambda^{-1}E^{-1}\tilde{U}_1,$$

where E is a matrix with lth column given by $\boldsymbol{\epsilon}_l$ and Λ is a diagonal matrix containing all the eigenvalues. Taking the inverse Laplace transform in time and inverse Fourier transform in space, we arrive at the boundary condition in the form of Eq. (17), with

$$\mathcal{F}_{j\to\mathbf{k}}\mathcal{L}_{t\to s}\boldsymbol{\alpha}_j(t)=E\Lambda^{-1}E^{-1}. \tag{35}$$

In this case, the boundary condition is exact in that it produces solutions as if the atoms on the left are still present.

It remains to show that for the kernels in Eq. (35), the reflection coefficient is zero. We change the variable s to $i\omega$, and $\lambda=e^{-id_n\xi}$. Then, by substituting Eq. (34) into Eq. (33), we find that ω is the frequency of the wave mode $\mathbf{k}+\xi\mathbf{n}$, with polarization vector $\boldsymbol{\epsilon}_l$. This implies that for any wave number $\mathbf{k}$,

$$A\boldsymbol{\epsilon}_s=e^{-id_n\xi}\boldsymbol{\epsilon}_s.$$

By comparing to the reflection matrix in Eq. (29), we see that the exact boundary condition, expressed via Fourier and Laplace transforms in Eq. (35), corresponds to zero reflection: $R(\mathbf{k})\equiv 0$.

For the one-dimensional example, setting $R(k)\equiv 0$ and using the dispersion relation, we obtain

$$\hat{\alpha}_0=e^{-ika_0}=1-\frac{m\omega^2}{4K^2}-i\frac{\sqrt{m}\omega}{2K}\sqrt{4-\frac{m\omega^2}{K^2}}. \tag{36}$$

Taking the inverse Laplace transform, we get

$$\alpha_0(t)=\frac{2}{t}J_2\left(\frac{2Kt}{\sqrt{m}}\right), \tag{37}$$

which is the same as the kernel obtained earlier [Eq. (23)].

IV. GOING BEYOND MORI-ZWANZIG

In the previous section, we have discussed an alternative characterization of the memory kernels using the reflection matrices: the exact memory kernels should lead to no reflection of outgoing phonons. Memory kernels that satisfy this condition are not unique. This opens up the possibility of extending the GLE models beyond the traditional Mori-Zwanzig framework. One benefit from such an extension is the added flexibility of choosing the memory kernels. As one application, we show later that the extended GLE formalism allows us to choose memory kernels that decay faster in time.

A. Extended generalized Langevin equation formalism

The kernels and noise term should satisfy the following conditions.

(1) The corresponding reflection coefficient is zero: $R(\mathbf{k})=0$ for all wave number.

(2) The fluctuation-dissipation theorem is satisfied.

For simplicity, we will illustrate the idea using the one-dimensional model,

$$\ddot{u}_j=u_{j+1}-2u_j+u_{j-1}.$$

We extend the GLE (21) to a set of GLEs with multiple memory and noise terms,

$$\ddot{u}_1=u_2-u_1-\sum_{j=1}^{J}\int_0^t\theta_{1j}(s)\dot{u}_j(t-s)ds+F_1(t),$$

$$\ddot{u}_2=u_3-2u_2+u_1-\sum_{j=1}^{J}\int_0^t\theta_{2j}(s)\dot{u}_j(t-s)ds+F_2(t),$$

$$\cdots$$

$$\ddot{u}_J=u_{J+1}-2u_J+u_{J-1}-\sum_{j=1}^{J}\int_0^t\theta_{Jj}(s)\dot{u}_j(t-s)ds+F_J(t),$$

$$\ddot{u}_{J+1}=u_{J+2}-2u_{J+1}+u_J,$$

$$\cdots. \tag{38}$$

To obtain the memory kernels, we set $k_BT=0$ so that the random noise terms drop out. The nonreflection condition implies that the system admits as exact solutions time harmonic waves of the form

$$u_j(t) = e^{i(jk-\omega t)},$$

with dispersion relation

$$\omega^2 = 2 - 2\cos k,$$

where we picked $k \in [-\pi, 0)$ and $\omega \geqslant 0$ so that the phase velocity is negative. The corresponding substitution yields

$$\begin{aligned} i\omega \sum_{j=1}^{J} \hat{\theta}_{1,j}(\omega) e^{-ijk} &= 1 - e^{-ik}, \\ \sum_{j=1}^{J} \hat{\theta}_{m,j}(\omega) e^{-ijk} &= 0, \end{aligned} \tag{39}$$

for $1 < m \leqslant J$. Here,

$$\hat{\theta}(\omega) = \int_0^\infty e^{-i\omega t}\theta(t)dt.$$

Using the dispersion relation, we can eliminate the wave number k from the equation above. In particular, we have

$$e^{ik} = 1 - \frac{\omega^2}{2} - \frac{i\omega}{2}\sqrt{4-\omega^2},$$

which will be subsequently denoted by $\beta(\omega)$. From Eq. (36), we see that β is exactly the Fourier transform of the memory kernel α_0 in Eq. (37). One can verify that α_0 decays like $t^{-3/2}$ over long time, and so does θ given by Eq. (22). This can be seen from $\beta(\omega)$, which has a square root singularity at $\omega = 2$,

$$\lim_{\omega \to 2-} \beta(\omega) = \infty.$$

B. Choosing memory kernels with faster decay rate

We will illustrate how we can take advantage of the added flexibility in choosing the memory kernels to obtain kernels with faster decay rate in time. We consider extended GLEs in the form

$$\begin{aligned} \ddot{u}_1 &= u_2 - u_1 - \int_0^t \theta_{11}(s)\dot{u}_1(t-s)ds \\ &\quad - \int_0^t \theta_{12}(s)\dot{u}_2(t-s)ds + F_1(t), \\ \ddot{u}_2 &= u_3 - 2u_2 + u_1 - \int_0^t \theta_{21}(s)\dot{u}_1(t-s)ds \\ &\quad - \int_0^t \theta_{22}(s)\dot{u}_2(t-s)ds + F_2(t), \\ \ddot{u}_j &= u_{j+1} - 2u_j + u_{j-1}. \end{aligned} \tag{40}$$

From Eqs. (39), we get

$$(1 - e^{-ik})\beta^2 = (-i\omega)[\hat{\theta}_{11}\beta(\omega) + \hat{\theta}_{12}]. \tag{41}$$

This equation can be simplified to

$$\hat{\theta}_{11}\beta(\omega) + \hat{\theta}_{12} = \frac{1}{2}(4-\omega^2)^{3/2} - \frac{3}{2}\sqrt{4-\omega^2} + \left(\frac{1}{2}\omega^3 - \frac{3}{2}\omega\right)i.$$

We now choose the kernels to remove the square root singularity. For example, one may choose the memory kernels whose Fourier transform take the following form:

$$(4-\omega^2)^{n/2} - iP(\omega),$$

where $P(\omega)$ is a polynomial which ensures that as ω approaches infinity, the function above converges to zero. For example, we can pick

$$\hat{\theta}_{11} = \frac{3}{8}(4-\omega^2)^{3/2} + \frac{3i}{8}(\omega^3 - 6\omega),$$

which, after an inverse Laplace transform, becomes

$$\theta_{11}(t) = \frac{9}{2t^3}[J_1(2t) - tJ_0(2t)].$$

This implies that

$$\begin{aligned} \hat{\theta}_{12} = \frac{1}{32}[&-3(4-\omega^2)^{5/2} + 10(4-\omega^2)^{3/2} \\ &+ 3\omega^5 i - 30\omega^3 i + 90\omega i], \end{aligned}$$

which, after an inverse Laplace transform, becomes

$$\theta_{12}(t) = \frac{15}{t^5}[(6t - t^3)J_0(2t) + (4t^2 - 6)J_1(2t)].$$

Clearly, these kernels decay like $t^{-5/2}$.

For the second GLE in Eq. (40), the substitution of the harmonic wave mode yields

$$\hat{\theta}_{21} + \hat{\theta}_{22}\left(1 - \frac{\omega^2}{2} + \frac{i\omega}{2}\sqrt{4-\omega^2}\right) = 0. \tag{42}$$

To remove the square root singularity, we may choose the kernel $\hat{\theta}_{22}(\omega)$ as follows:

$$\hat{\theta}_{22}(\omega) = (4-\omega^2)^{3/2} + i(\omega^3 - 6\omega) + q(\omega),$$

where the additional function $q(\omega)$ is smooth and behaves as

$$q(\omega) \sim 8i/\omega$$

near $\omega = \pm 2$. Obviously, $\theta_{22}(\omega)$ decays no slower than $t^{-5/2}$. In addition, one can verify that

$$\lim_{\omega \to 2} \hat{\theta}_{22}(\omega) = 0, \quad \lim_{\omega \to 2} \hat{\theta}'_{22}(\omega) < +\infty,$$

which implies that $\hat{\theta}_{21}(\omega)$ has finite first derivative. Hence, $\theta_{21}(t)$ has a faster decay than θ given by Eq. (22). Therefore, by extending the system in space, we obtain kernels that decay faster in time.

C. Fluctuation-dissipation theorem for the extended generalized Langevin equations

We will briefly discuss the fluctuation-dissipation theorem for the extended GLEs. Consider a set of linear GLEs,

$$m\ddot{\mathbf{u}} = B\mathbf{u} - \int_0^t \theta(s)\dot{\mathbf{u}}(t-s)ds + F(t). \tag{43}$$

Here, $\mathbf{u}$ is a vector representing the displacement of all the particles in D. B is a constant matrix. We will assume that the random noise is uncorrelated with the initial velocity,

$$\langle F(t)\dot{\mathbf{u}}(0)^T\rangle = 0. \tag{44}$$

The Gibbs distribution for the system can be expressed in the form

$$\frac{1}{Z}e^{-\beta[(1/2)m\mathbf{v}^2+(1/2)\mathbf{u}^T A\mathbf{u}]}, \tag{45}$$

where $\mathbf{v}=\dot{\mathbf{u}}$ is the velocity or momentum. We note that the choice of the Gibbs distribution might be an issue by itself. The quadratic form $\mathbf{u}^T A\mathbf{u}$ represents the potential energy of the system and should take into account the effect of the boundary condition. This issue arises already in the context of static problems at zero temperature. In particular, it arises in quasicontinuum method.[31] Failure to account correctly for the boundary conditions in the matrix A results in ghost forces. This has been discussed in Ref. 32. This also provides the point of contact between the boundary conditions for the static and dynamic problems.

Define

$$\psi(t) = \langle \mathbf{u}(t)\mathbf{u}(0)^T\rangle. \tag{46}$$

From Eq. (45), the initial values of ψ are given by

$$\psi(0) = k_B T A^{-1}, \quad \psi'(0) = 0, \quad \psi''(0) = -k_B T I, \quad \psi'''(0) = 0. \tag{47}$$

Multiplying the first equation in Eq. (43) by $\mathbf{v}(0)^T$ and applying Laplace transform in time, we get

$$\tilde{\psi}(\lambda) = [-m\lambda^3 - \lambda^2\tilde{\theta} + \lambda B]^{-1} \times\{[-m\lambda^2\psi(0) - \lambda\tilde{\theta}\psi(0) + B\psi(0)] + mk_B T I\}. \tag{48}$$

Now, we can compute the time correlation of the random noise. We rewrite the GLE as

$$F(t) = m\ddot{\mathbf{u}} - B\mathbf{u} + \int_0^t \theta(s)\dot{\mathbf{u}}(t-s)ds,$$

and calculate the Laplace transform of the time correlation of the random noise using the formula for ψ. This leads to

$$\langle F(t)F(0)^T\rangle = \mathcal{F}^{-1}\left\{k_B T\tilde{\theta} + \frac{1}{\lambda}[B\psi(0) + k_B T]B^T\right\} = k_B T[\theta(t) + (BA^{-1} + I)B^T]. \tag{49}$$

In particular, if $B=-A$, we have

$$\langle F(t)F(0)^T\rangle = k_B T\theta(t).$$

Equation (49) provides a generalized fluctuation-dissipation theorem that has to be satisfied in order for the system to equilibrate to the right Gibbs distribution.

V. APPROXIMATION OF THE GENERALIZED LANGEVIN EQUATIONS

We have shown that the memory kernels can be found by setting the reflection coefficient to zero. However, in practice, these boundary conditions can be quite awkward since all boundary atoms are coupled together and the memory kernels decay rather slowly. For an $N\times N\times N$ system, if the memory integrals over time are truncated beyond M time steps, then the total cost of updating the position of one boundary atom is $O(MN^2)$ if direct summation is used. One might be able to develop fast summation techniques, as is the case with influence matrix techniques in numerical simulation of wave propagation[33] or fluid dynamics.[34]

We will pursue a different path: We will discuss how one can find approximate boundary conditions which are effectively local. The fact that this is possible is suggested by the discussions in the previous section. Such approximate boundary conditions are more flexible in practice, especially for systems with realistic geometries and for problems in which the computational region has to move, for example, to follow defects.[2,3] From a philosophical viewpoint, this also serves as an example that illustrates how we can make efficient approximations to the Mori-Zwanzig formalism.

A. General principle

The construction of the approximate boundary conditions will be based on the following principles.

(1) Efficiency: The boundary condition should preferably be local and it should not lead to too much computational overhead.

(2) Accuracy: Given the allowed computational cost, here in the form of the size of the stencils (to be defined later), we will find approximations to the exact boundary condition (11) with optimal accuracy. In this sense, what is done here resembles the philosophy behind optimal prediction.[20]

(3) Stability: The approximate boundary conditions should be numerically stable. This will constrain the approximate kernels to be positive definite.

We will seek approximate kernels within the class of functions that are local. In this case, the memory terms become of the form

$$\sum_j \int_0^{t_0} \boldsymbol{\theta}_{i-j}(s)\dot{\mathbf{u}}_j(t-s)ds,$$

with a finite summation over j. Here, t_0 specifies the length of the time history that we allow the boundary atoms to depend on. This is equivalent to replacing the kernels in Eq. (17) by local ones,

$$\mathbf{u}_0(t) = \sum_{\mathbf{r}_j\in J}\int_0^{t_0} \boldsymbol{\alpha}_j(s)\mathbf{u}_j(t-s)ds. \tag{50}$$

Here and in the following, we will index the boundary atoms by a subscript 0. Recall that $J_1=\{j:\mathbf{r}_j\cdot\mathbf{n}=d_n\}$. We let $J\subset\{j:\mathbf{r}_j\cdot n>0\}$ to be a set of preselected neighboring lattice points in the interior. The sets $J\times(0,t_0)$ or $J\times\{m=1,2,\ldots,M\}$ are called the *stencil*, a terminology that is

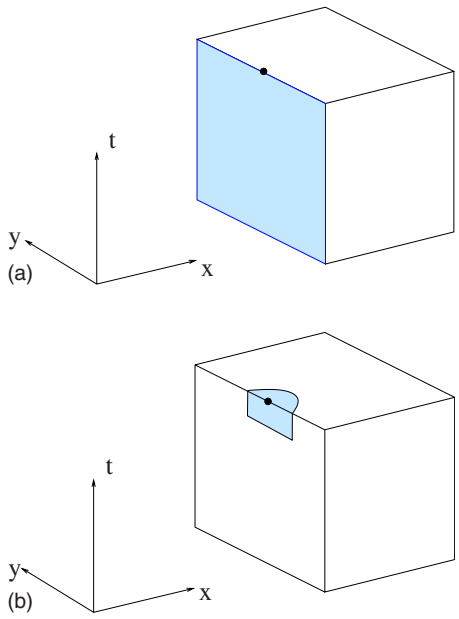

FIG. 4. (Color online) Domain of dependence for the exact boundary conditions (top) and the local boundary conditions (bottom). The filled circle represents an atom at the boundary, and the shaded areas indicate the domain of dependence. The normal direction of the boundary is aligned along the x axis.

often used in the numerical computation of solutions of partial differential equations. By selecting the stencils, we restrict the kernels to local functions. Namely,

$$\boldsymbol{\alpha}_j(t) = 0 \quad \text{for } j \notin J \quad \text{or } t > t_0. \tag{51}$$

Another way to think about boundary conditions in the form of Eqs. (17) and (50) is to view them as a way of specifying the positions of the bath atoms that lie within the interaction range of the atoms in the computational domain and, in particular, what the positions of these atoms depend on. This is similar to the notion of domain of dependence in the context of partial differential equations. For the exact boundary condition, the domain of dependence is the entire plane next to the boundary, i.e., the set J_1. For the approximate boundary condition, however, it is much more local as shown in Fig. 4 for a two-dimensional system.

The memory kernels $\boldsymbol{\theta}_j$ and $\boldsymbol{\alpha}_j$ are related as follows:

$$\boldsymbol{\theta}_j(t) = -\sum_{k \in J_1} D_k \int_t^{+\infty} \boldsymbol{\alpha}_{j+k}(s) ds. \tag{52}$$

This is proved in Appendix B.

In the discrete form, the boundary condition we are looking for becomes

$$\mathbf{u}_0^{n+1} = \sum_{j \in J} \sum_{m=1}^{M} \boldsymbol{\alpha}_j^m \mathbf{u}_j^{n-m+1} \Delta t. \tag{53}$$

The number of points in J and the number of time steps M determine the cost of implementing such boundary condition. Given the stencil, our aim is to find optimal boundary conditions of the form discussed above, by choosing the matrices $\{\boldsymbol{\alpha}_j\}$ or $\{\boldsymbol{\theta}_j\}$ in the right way. For now, we will again limit ourselves to the case when the computational domain is half space and we will assume that the approximate boundary conditions are translation invariant. In the continuous form, the boundary condition for the other atoms at the boundary takes the form

$$\mathbf{u}(\mathbf{r}_i, t) = \sum_{j \in J} \int_0^{t_0} \boldsymbol{\alpha}_j(s) \mathbf{u}(\mathbf{r}_i + \mathbf{r}_j, t - s) ds. \tag{54}$$

B. Variational formulation of the exact kernels

Given a set of kernels in the proposed boundary condition, one may define the total reflection as

$$E[\{\boldsymbol{\alpha}_j\}; \mathbf{n}] = \sum_s \sum_{s'} \int |R_{ss'}|^2 W_s(\mathbf{k}) d\mathbf{k}, \tag{55}$$

where $W_s(\mathbf{k}) \geqslant 0$ is some weight function. Here, the dependence of the right hand side on the kernels enters through the reflection matrices $R_{ss'}$. In the previous section, we have shown that for the exact memory kernels, the corresponding reflection coefficient must be zero. In other words, the exact kernels form a minimizer of the functional E.

There are many natural choices of the weight function W. In Refs. 2 and 3, W is taken to be a constant. In Ref. 5, W is taken as

$$W_s(\mathbf{k}) = |\nabla \omega_s(\mathbf{k}) \cdot \mathbf{n}|. \tag{56}$$

In this case, Eq. (55) represents the energy flux across the boundary due to the reflection of phonons. One can also restrict the integration domain in the wave number space to the subset of the first Brillouin zone B that corresponds to the incident wave. The functional then becomes

$$E[\{\boldsymbol{\alpha}_j\}; \mathbf{n}] = \sum_s \sum_{s'} \int_{\mathbf{k} \in B, \mathbf{k} \cdot \mathbf{n} \leqslant 0} |R_{ss'}|^2 W_s(\mathbf{k}) d\mathbf{k}. \tag{57}$$

C. Approximate memory kernels

Motivated by the variational formulation of the exact kernels, we will find the approximate kernels by minimizing the functional I, in the class of kernels that satisfy Eq. (51). To ensure accuracy for long wavelength modes, we impose the constraint that $R(0)=0$, which leads to

$$\sum_{j \in J} \int_0^{\infty} \boldsymbol{\alpha}_j(s) ds = I, \tag{58}$$

where I is the $d \times d$ identity matrix. For complex lattices, since the phonon spectrum has optical branches, this constraint has to be modified. Let

$$K = \begin{pmatrix} I \\ I \\ \vdots \\ I \end{pmatrix}$$

be a $dn_a \times d$ matrix. Then, the constraint can be written as

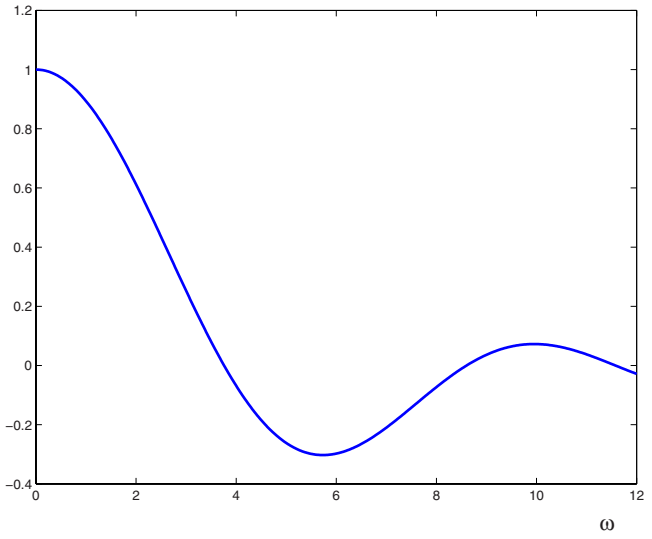

FIG. 5. (Color online) The Fourier transform of an approximate boundary condition obtained by minimizing the total reflection.

$$\sum_{j\in J}\int_0^\infty \boldsymbol{\alpha}_j(s)dsK = K. \tag{59}$$

Once $\boldsymbol{\alpha}_j$ is computed, we obtain $\boldsymbol{\theta}_j$ from Eq. (52). Alternatively, one can directly use $\boldsymbol{\theta}_j(t)$ as the variables in the variational formulation, and solve the optimization problem

$$E[\{\boldsymbol{\theta}_j\};\mathbf{n}] = \sum_s \int_{\mathbf{k}\in B,\mathbf{k}\cdot\mathbf{n}\leqslant 0} \sum_{s'} |R_{ss'}|^2 W_s(\mathbf{k})d\mathbf{k}. \tag{60}$$

Using Eq. (52), the constraint (59) becomes

$$\sum_j \boldsymbol{\theta}_j(0)K = -\sum_{k\in J_1} D_k K. \tag{61}$$

The stability condition requires that the Fourier transform of $\boldsymbol{\theta}_j$, known as the power spectrum, be semipositive definite, i.e., all eigenvalues must be non-negative. The solution to the variational problem discussed above does not automatically guarantee this property. For instance, for the one-dimensional model, Fig. 5 shows the Fourier transform of an approximate boundary condition, which is computed from the variational approach using α as the variable. Clearly, the Fourier transform becomes negative as the frequency gets high enough. Although the power spectrum stays positive for $\omega < \omega_{max}$, with $\omega_{max}=2$, which is the highest frequency for the phonons in this system, instability may develop over long time integrations.

To guarantee stability, we seek the memory kernels $\boldsymbol{\theta}_j(t)$ that have the following form:

$$\boldsymbol{\theta}_j(t) = \sum_p \int_{-t_0}^{t_0} \Gamma_p(s)\Gamma_{j+p}(t+s)^T ds, \tag{62}$$

or in discrete form,

$$\boldsymbol{\theta}_j^n = \sum_{p,m} \Gamma_p^m (\Gamma_{j+p}^{n+m})^T \Delta t. \tag{63}$$

This guarantees that the stability condition is satisfied. To see this, let $\Theta(\mathbf{k},\omega)$ and $\hat{\Gamma}(\mathbf{k},\omega)$ be the Fourier transform in time and on the tangent plane for $\boldsymbol{\theta}$ and Γ, respectively. Then,

$$\Theta(\mathbf{k},\omega) = \hat{\Gamma}(\mathbf{k},\omega)\hat{\Gamma}(\mathbf{k},\omega)^*,$$

which guarantees the semipositive definiteness. Furthermore, in order for $\boldsymbol{\theta}_j$ to be a correlation function as is stipulated by the fluctuation-dissipation theorem [Eq. (16)], one must have

$$\boldsymbol{\theta}_j(t) = \boldsymbol{\theta}_{-j}(-t)^T.$$

This is automatically satisfied with Eq. (62).

Now, we change the variables in the variational formulation to $\Gamma_j(t)$ and we solve the problem

$$\min_{\{\Gamma_j\}} E[\{\Gamma_j\};\mathbf{n}]. \tag{64}$$

Once $\Gamma_j(t)$ is obtained from the variational principle, we compute $\boldsymbol{\theta}_j(t)$ using Eq. (62).

These approximate boundary conditions were referred to as VBCs in Ref. 5. They provide a good compromise between accuracy and complexity. It has been demonstrated[5] that with VBC, one can achieve almost the same accuracy as the exact boundary conditions, at a much lower cost. Other implementation issues as well as comparison with other boundary conditions are discussed in Ref. 35.

D. Sample the random noise

Once the memory kernels are available, we can sample the random force using the fluctuation-dissipation relation

$$\langle F_i(t)F_j(0)^T\rangle = k_B T\boldsymbol{\theta}_{i-j}(t). \tag{65}$$

We first show how to find $F_i(t)$ analytically. Taking a Fourier transform in time, we get

$$\hat{F}_j(\omega) = \int_{-\infty}^{\infty} F_j(t)e^{-i\omega t}dt.$$

Obviously, the Fourier coefficient $\hat{F}_i(\omega)$ is a Gaussian random variable for every ω. To find the correlation, we make a substitution of the equation above to Eq. (65), and we find

$$\langle \hat{F}_i(\omega_1)\hat{F}_j(\omega_2)^T\rangle = k_B T\hat{\boldsymbol{\theta}}_{i-j}(\omega_1)\delta(\omega_1+\omega_2),$$

where

$$\hat{\boldsymbol{\theta}}_j(\omega) = \int_{-\infty}^{\infty} \boldsymbol{\theta}_j(t)e^{-i\omega t}dt. \tag{66}$$

Therefore, after the Fourier transform, the random noise is uncorrelated. For the spatial correlation, we perform a Fourier transform along the boundary. Let

$$\mathcal{F}(\mathbf{k},\omega) = \sum_{j\in J_1} \hat{F}_j(\omega)e^{-i\mathbf{r}_j\cdot\mathbf{k}}. \tag{67}$$

For any wave number $\mathbf{k}$, such that $\mathbf{k}\cdot\mathbf{n}=0$, $\mathcal{F}(\mathbf{k},\omega)$ is a stationary Gaussian process. Using the identity in Eq. (65) and the stationarity in space, we obtain

$$\langle \mathcal{F}(\mathbf{k}_1,\omega_1)\mathcal{F}(\mathbf{k}_2,\omega_2)^T\rangle = k_B T\Theta(\mathbf{k}_1,\omega_1)\delta(\mathbf{k}_1+\mathbf{k}_2)\delta(\omega_1+\omega_2), \tag{68}$$

where

$$\Theta(\mathbf{k},\omega) = \sum_{j\in J_1} \hat{\boldsymbol{\theta}}_j(\omega)e^{-i\mathbf{r}_j\cdot\mathbf{k}}.$$

The matrix Θ, known as the *power spectrum*, provides the covariance matrix for the Fourier coefficients of the random noise. The random processes are completely determined by their power spectrum. This procedure can be implemented numerically to sample the Gaussian noise.[36–38]

The specific form in Eq. (62), however, makes this step quite easy. Let $W_p(t)$ be a sequence of independent white noises,

$$\langle W_p(t)W_q(0)^T\rangle = \delta_{pq}\delta(t).$$

Let

$$F_j(t) = \sqrt{k_B T}\sum_p \int_0^{t_0} \Gamma_p(s)W_{j+p}(t+s)ds. \tag{69}$$

Then, $F_j(t)$ is a Gaussian process satisfying

$$\langle F_j(t)F_0(0)^T\rangle = k_B T\boldsymbol{\theta}_j(t).$$

In discrete form, let W_p^m be a sequence of independent identically distributed normal random variables. Then,

$$F_j^n = \sum_{p,m} \sqrt{k_B T\Delta t}\Gamma_p^m W_{j+p}^{n+m}.$$

E. Overall algorithm

The overall algorithm consists of the following steps.

(1) Generate quadrature points in the first Brillouin zone in order to perform the integration in Eq. (60). Here, the k-point method[39] is used.

(2) Compute the dispersion relation and the polarization vectors at each quadrature point.

(3) For each quadrature point $\mathbf{k}$, such that $\mathbf{k}\cdot\mathbf{n}\leqslant 0$, find all possible wave numbers for the reflected phonon, $\{\mathbf{k}_{ss'}^R, s' = 1,2,\ldots,N_R\}$, as well as the corresponding polarization vectors.

(4) Select the stencil, i.e., the set J and the number of time steps M.

(5) Initialize the time history kernels $\{\Gamma_j^m\}$.

(6) Compute the reflection coefficients $R_{ss'}$ from Eqs. (29), (52), and (62).

(7) Compute the objective function from Eq. (60).

(8) Use an optimization routine to obtain new values for the kernels Γ_j^m. The BFGS subroutine[40] is used here.

(9) Go to step 6 unless certain convergence criterion is met.

After the kernels Γ_j^m are computed from the variational formulation, we find $\boldsymbol{\theta}_j$ from Eq. (62) and sample the random forces from Eq. (69). All these are done in a precomputing step, namely, we precompute the kernels and the random force and store the data for later use. In the MD simulation, we add the memory and the random force terms to atoms at the boundary at each time step.

F. Error analysis

To analyze the error we make in approximating the kernels $\boldsymbol{\alpha}_j$, we take the Fourier transform

$$\mathcal{A}(\mathbf{k},\omega) = \sum_{j\in J_1} \int_0^\infty \boldsymbol{\alpha}_j(t)e^{-i(\mathbf{k}\cdot\mathbf{r}_j+\omega t)}dt. \tag{70}$$

For the exact memory kernels, this is denoted by $\mathcal{A}_0(\mathbf{k},\omega)$. Similarly, we define the Fourier transform of the kernels $\boldsymbol{\theta}_j$,

$$\Theta(\mathbf{k},\omega) = \sum_{j\in J_1} \int_0^\infty \boldsymbol{\theta}_j(t)e^{-i(\mathbf{k}\cdot\mathbf{r}_j+\omega t)}dt, \tag{71}$$

and denote the exact power spectrum by Θ_0. We also define

$$\hat{D}(\mathbf{k}) = \sum_{j\in J_1} D_{-m}e^{-i\mathbf{k}\cdot\mathbf{r}_j}.$$

In order to estimate the magnitude of the error, we recall some notations for matrix norms. We will use $|\cdot|$ to denote the length for vectors. For an $n\times n$ matrix B, we will use the l_2 and l_∞ norms, given by

$$\|B\|_2 = \sqrt{\lambda_{\max}(B^TB)}, \quad \|B\|_\infty = \max_i \sum_j |B_{ij}|,$$

where $\lambda_{\max}(B^TB)$ is the largest eigenvalue of the matrix B^TB.

We will show the following.

Theorem V.1. The error in approximating $\mathcal{A}_0(\mathbf{k},\omega)$ is controlled by the magnitude of the reflection coefficients. More specifically, we have

$$\|\mathcal{A}(\mathbf{k},\omega)-\mathcal{A}_0(\mathbf{k},\omega)\|_2 \leqslant \frac{[1+\|\mathcal{A}_0(\mathbf{k},\omega)\|_2]\sqrt{S}\|R(\mathbf{k},\omega)\|_\infty}{1-\sqrt{S}\|R(\mathbf{k},\omega)\|_\infty} \tag{72}$$

and

$$\|\Theta(\mathbf{k},\omega)-\Theta_0(\mathbf{k},\omega)\|_2 \leqslant \frac{\|\hat{D}(\mathbf{k})\|_2[2+\|\mathcal{A}_0(\mathbf{k},\omega)\|_2+\|\mathcal{A}_0(\mathbf{k},0)\|_2]\sqrt{S}\|R(\mathbf{k},\omega)\|_\infty}{\omega(1-\sqrt{S}\|R(\mathbf{k},\omega)\|_\infty)}, \tag{73}$$

provided that $\sqrt{S}\|R\|_\infty < 1$. Here, S is the number of phonon branches of the system.

In order to relate $\mathcal{A}$ to the matrix A in Eq. (29) for the reflection matrix, we define for any $\mathbf{k} \in J_0$ and $\omega > 0$ the normal components η_s^I and $\eta_{ss'}^R$ such that the frequency is matched,

$$\omega_s(\boldsymbol{\xi}) = \omega_{s'}(\eta_{ss'}^R \mathbf{n} + \mathbf{k}) = \omega, \quad \boldsymbol{\xi} = \eta_s^I \mathbf{n} + \mathbf{k}.$$

In addition, to represent the incidence and reflection modes, we require

$$\mathrm{Im}(\eta_s^I) \leqslant 0, \quad \mathrm{Im}(\eta_{ss'}^R) \geqslant 0.$$

Then, $\boldsymbol{\xi} \cdot \mathbf{r}_j + \omega_s t = \mathbf{k} \cdot \mathbf{r}_j + \omega t + d_n \eta_s^I$. Therefore,

$$\mathcal{A}(\mathbf{k}, \omega) = \bar{A}(\boldsymbol{\xi}) e^{-i d_n \eta_s^I}.$$

Let $\boldsymbol{\varepsilon}_{ss'} = \boldsymbol{\varepsilon}_{s'}(\eta_{ss'}^R \mathbf{n} + \mathbf{k})$. We change the variable to $(\mathbf{k}, \omega)$ and rewrite the Eq. (29) for the reflection matrix as

$$(I - e^{i d_n \eta_s^I} \mathcal{A}) \boldsymbol{\varepsilon}_s + \sum_{s'} R_{ss'} (I - e^{i d_n \eta_{ss'}^R} \mathcal{A}) \boldsymbol{\varepsilon}_{ss'} = 0. \quad (74)$$

Now, we define the matrices E^I, E^R, $\tilde{E}^I$, and $\tilde{E}^R$ whose sth columns are

$$E_s^I = \boldsymbol{\varepsilon}_s, \quad E_s^R = \sum_{s'} R_{ss'} \boldsymbol{\varepsilon}_{ss'},$$

$$\tilde{E}_s^I = e^{i d_n \eta_s^I} \boldsymbol{\varepsilon}_s, \quad \tilde{E}_s^R = \sum_{s'} R_{ss'} e^{i d_n \eta_{ss'}^R} \boldsymbol{\varepsilon}_{s'}.$$

We then have

$$\mathcal{A}(\mathbf{k}) = (E^I + E^R)(\tilde{E}^I + \tilde{E}^R)^{-1}.$$

In particular,

$$\mathcal{A}_0 = E^I (\tilde{E}^I)^{-1},$$

for the exact boundary condition. By subtracting $\mathcal{A}_0$ from $\mathcal{A}$, we have

$$\mathcal{A} - \mathcal{A}_0 = (E^R - \mathcal{A}_0 \tilde{E}^R)(\tilde{E}^I + \tilde{E}^R)^{-1}. \quad (75)$$

Since the dynamic matrix is symmetric, one can choose orthonormal eigenvectors for $\boldsymbol{\varepsilon}_s$. Therefore, $\|E^I\|_2 = 1$. In addition, we have

$$|E_s^R| \leqslant \sum_{s'} |R_{ss'}| \leqslant \|R\|_\infty,$$

which implies that

$$\|E^R\|_2 \leqslant \sqrt{S}\|R\|_\infty. \quad (76)$$

Similarly, one can show that

$$\|\tilde{E}^R\|_2 \leqslant \sqrt{S}\|R\|_\infty. \quad (77)$$

The matrix inverse in Eq. (75) exists if

$$\|\tilde{E}^R\|_2 < 1.$$

This is the case if $\|R\|_\infty < 1/\sqrt{S}$. In addition, we have

$$\|(\tilde{E}^I + \tilde{E}^R)^{-1}\|_2 \leqslant \frac{1}{1 - \|\tilde{E}^R\|_2} \leqslant \frac{1}{1 - \sqrt{S}\|R\|_\infty}. \quad (78)$$

Combining Eqs. (75)–(78), we arrive at Eq. (72).

A similar estimate can be established for $\boldsymbol{\theta}_j$. This will also determine the accuracy in computing the random forces. With Eq. (52), we further relate Θ to $\mathcal{A}$,

$$\Theta(\mathbf{k}, \omega) = (-i\omega)^{-1} \hat{D}[\mathcal{A}(\mathbf{k}, \omega) - \mathcal{A}(\mathbf{k}, 0)]. \quad (79)$$

This formula shows how to compute the power spectrum from the applied boundary condition (50). Combining Eqs. (72) and (79), we get the estimate for the power spectrum in Eq. (73).

For the one-dimensional example discussed earlier, we have from Eq. (31)

$$\hat{\alpha} = \frac{1 + R}{e^{ika_0} + R e^{-ika_0}}.$$

Meanwhile, from Eq. (52) and the constraint (58), we get

$$\hat{\theta}(\omega) = K(i\omega)^{-1}(1 - \hat{\alpha}), \quad \hat{\theta}_0(\omega) = K(i\omega)^{-1}(1 - \hat{\alpha}_0). \quad (80)$$

Therefore,

$$\hat{\theta} - \hat{\theta}_0 = -KR(1 - e^{-2ika_0})[(e^{ika_0} + R e^{-ika_0})(i\omega)]^{-1}, \quad (81)$$

for $k \in \left(-\frac{\pi}{a_0}, 0\right)$ and $0 \leqslant \omega/K \leqslant 2$.

The equation above expresses the error for the power spectrum in terms of the reflection coefficients. In particular, it shows that a boundary condition with small reflection coefficient also provides a good approximation for the power spectrum.

VI. EXAMPLES

A. One-dimensional chain with nearest neighbor interaction

Here, we consider a one-dimensional chain with nearest neighbor Lennard-Jones interaction [Eq. (19)]. As demonstrated in Sec. II, the exact boundary condition for this simple model can be found analytically and is given in Eq. (22). Since m, σ, and ϵ can be used as the unit for mass, length, and energy, respectively, they are taken to be unity in our computation, and all the following numerical results are presented in terms of the reduced unit. For instance, the unit for time is given by $\tau = \sigma\sqrt{m/\epsilon}$. For the time integration, the time step is taken to be $\Delta t = 0.0132\tau$.

For this one-dimensional model, various numerical experiments have been conducted at zero temperature, which have demonstrated the ability of VBC to prevent wave reflection at the boundary.[2,3,5] Here, we focus our attention on finite temperature VBC. We first consider the power spectrum obtained from the history kernel via Eq. (52). From the exact kernel in Eq. (22), one can show that for the exact boundary condition, the power spectrum is given by

$$\hat{\theta}_0(\omega) = \sqrt{1 - \omega^2/4}, \quad \omega \in [0, 2].$$

In Fig. 6, $\hat{\theta}_0$ is plotted together with the power spectrum computed from the VBC with $M = 20$. One can see that even

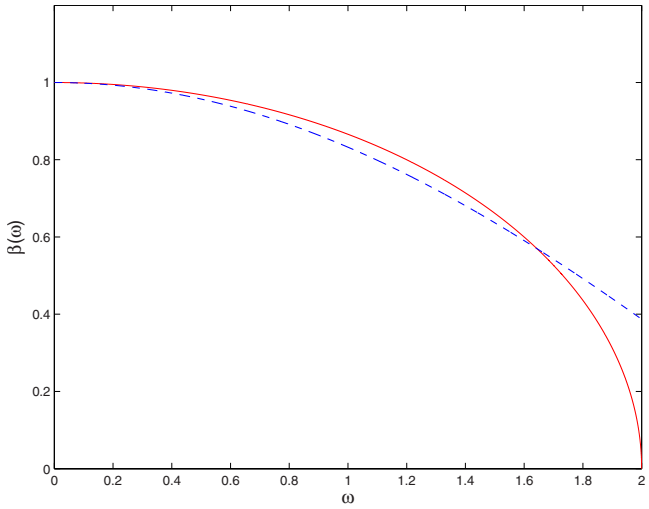

FIG. 6. (Color online) Comparison of the power spectrum. Solid line: Power spectrum from the exact boundary condition. Dashed line: Power spectrum computed from VBC with $M=20$.

though VBC only includes a small number of history data, it provides a fairly accurate approximation of the power spectrum. As the frequency ω approaches 2, which is the maximum phonon frequency, the discrepancy becomes bigger.

One application of the boundary conditions developed here is to use it as a thermostat. Compared with existing thermostats such as the Andersen and Nosé-Hoover thermostats, the thermostat proposed here has the attractive feature that it is derived from a rather physical setup, through the use of heat bath atoms and then eliminating the bath atoms. The effect of the heat bath is represented in the boundary conditions—the dynamics of the interior atoms is not disturbed directly.

We will examine the application of the VBCs as thermostats. We consider a system consisting of 200 atoms. The system is initially at rest, and then integrated for 200 000 time steps with the VBCs applied to the first and the last atoms at a constant temperature $k_BT=0.001$. Figure 7(a) shows the measured system temperature for each step of the time integration. Here, the system temperature is defined as the mean kinetic energy per particle,

$$k_B\tilde{T} = \frac{1}{N}\sum_{j=1}^{N} v_i^2.$$

After about 25 000 time steps, the system is brought to the applied temperature. This relaxation time depends on the system size.

To see how dynamics is accurately produced, we computed the velocity autocorrelation function

$$C(t) = \langle v_i(t)v_i(0)\rangle.$$

For comparison, we conducted a separate microcanonical simulation with periodic boundary condition applied. The system is prepared with a simulation of the canonical ensemble at the same temperature with Nosé-Hoover thermostat.[41,42] Once the system has equilibrated, we turn off

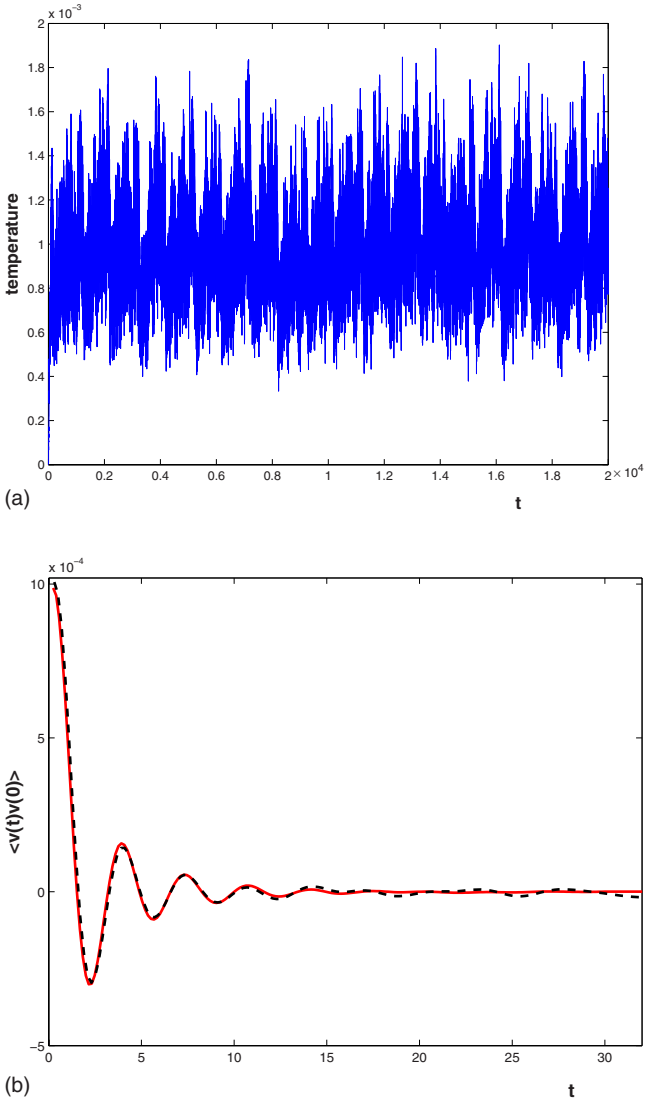

FIG. 7. (Color online) Molecular dynamics simulation in a one-dimensional Lennard-Jones system with variational boundary conditions applied: (a) system temperature and (b) velocity correlation. Solid line: Velocity correlation computed from a separate microcanonical MD simulation with the same temperature. Dashed line: Velocity correlation computed from the MD simulation with finite temperature VBC applied.

the thermostat and start sampling the time correlation. The purpose of this step is to eliminate changes of the velocity autocorrelation function due to thermostating. The velocity correlation obtained from this procedure is considered to be "exact." In Fig. 7(b), these velocity correlation functions are shown. We see that with a small stencil $M=20$, the finite temperature VBC reproduces quite accurately the time correlation function.

One special case of the GLE (21) is the regular Langevin equation,

$$\ddot{u}_1 = \phi'(x_2 - x_1) - \frac{1}{2}\dot{u}_1 + F_i(t). \tag{82}$$

This corresponds to choosing a singular memory kernel $\theta(t)=\delta(t)$ and $F_i(t)$ to be the white noise. This type of models

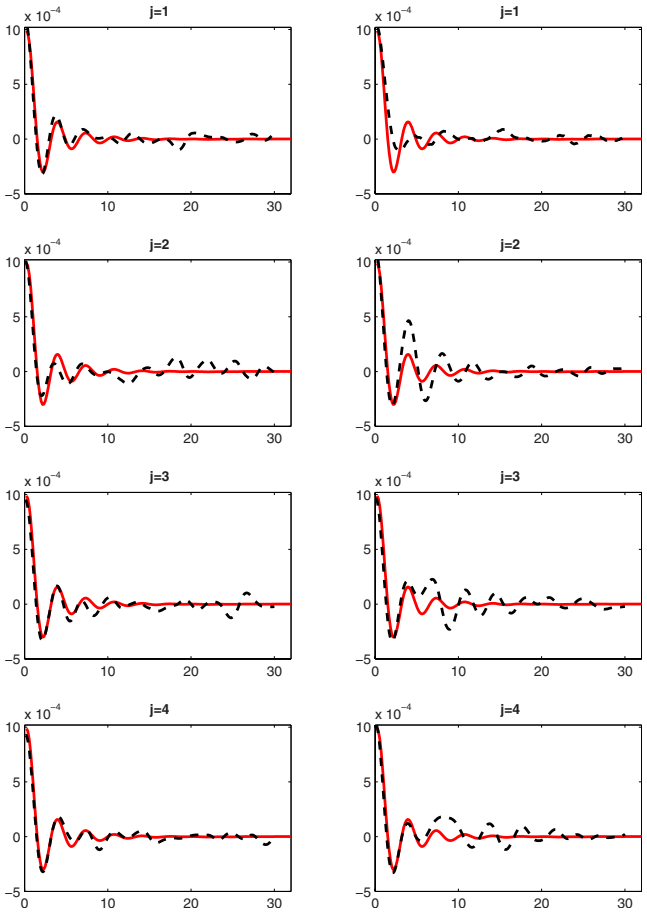

FIG. 8. (Color online) The velocity autocorrelation function for atoms near the boundary. The simulation is conducted with VBC applied at the boundaries. Solid lines: Results from simulation for the microcanonical ensemble. Dashed line: Results using various versions of the VBC. Left: Results of VBC with 20 time steps involved in the boundary condition ($M=20$). Right: Only one time step is involved, which corresponds to the regular Langevin equation (82). From top to bottom: The velocity autocorrelation functions for the first to the fourth atoms next to the boundary.

has been quite popular in molecular dynamics simulations at finite temperature. They have also been used as boundary conditions to absorb elastic waves and introduce thermal noise.[43,44] However, such boundary conditions do not produce the correct time correlation functions, especially for atoms near the boundary. This is shown in Fig. 8 where we plotted the velocity autocorrelation function computed from a simulation with boundary condition (82) applied at the boundary. These results are compared to the correct correlation functions and the results from a VBC with a bigger stencil, $M=20$. One can see that even though the system has been brought to an equilibrium consistent with the applied temperature, indicated by the correct value of the correlation function at $t=0$, the velocity autocorrelations for $t>0$ do not quite agree with the correct values. The discrepancy, however, will diminish as one moves into the interior. For the VBC with a bigger stencil, $M=20$, the results are quite good even for the atoms near the boundary. These phenomena have also been observed in other examples that we have studied.

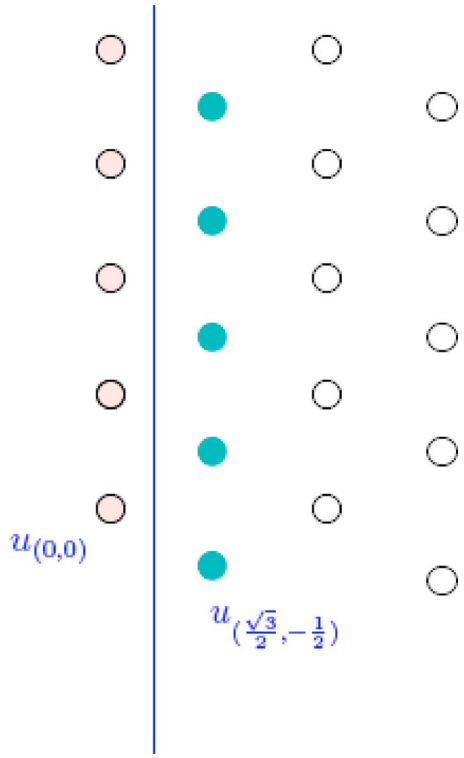

FIG. 9. (Color online) Two-dimensional triangular lattice: the solid line indicates the location of the boundary, and the filled circles are the atoms at the boundary. The subscripts indicate the lattice point. The first and second subscripts indicate the location of the lattice points in the horizontal and vertical directions, respectively, in the units of the lattice constant a_0.

B. Two-dimensional triangular lattice

Next, we consider a two-dimensional triangular lattice. The atomic potential is again given by the Lennard-Jones potential with nearest neighbor interaction. The lattice parameter is $a_0=\sqrt[6]{2}\sigma$ with a cut-off distance $r_c=1.7a_0$. Figure 9 shows the crystal structure near the boundary with normal $\mathbf{n}=(1,0)$. For this system, the force constant for the lattice point $\mathbf{r}$ is given by

$$D_{\mathbf{r}}=\frac{\phi''(a_0)}{a_0^2}\mathbf{r}\otimes\mathbf{r}.$$

The boundary condition for the first layer of atoms outside the boundary can be written as

$$\mathbf{u}_{(0,i)}=\sum_{j=-N+1/2}^{N-1/2}\int_0^t \boldsymbol{\alpha}_j(s)\mathbf{u}_{(\sqrt{3}/2,i+j)}(t-s)ds.$$

There are $2N$ atoms involved in this boundary condition. The exact boundary condition would require $N=+\infty$.

From Eq. (52), we get

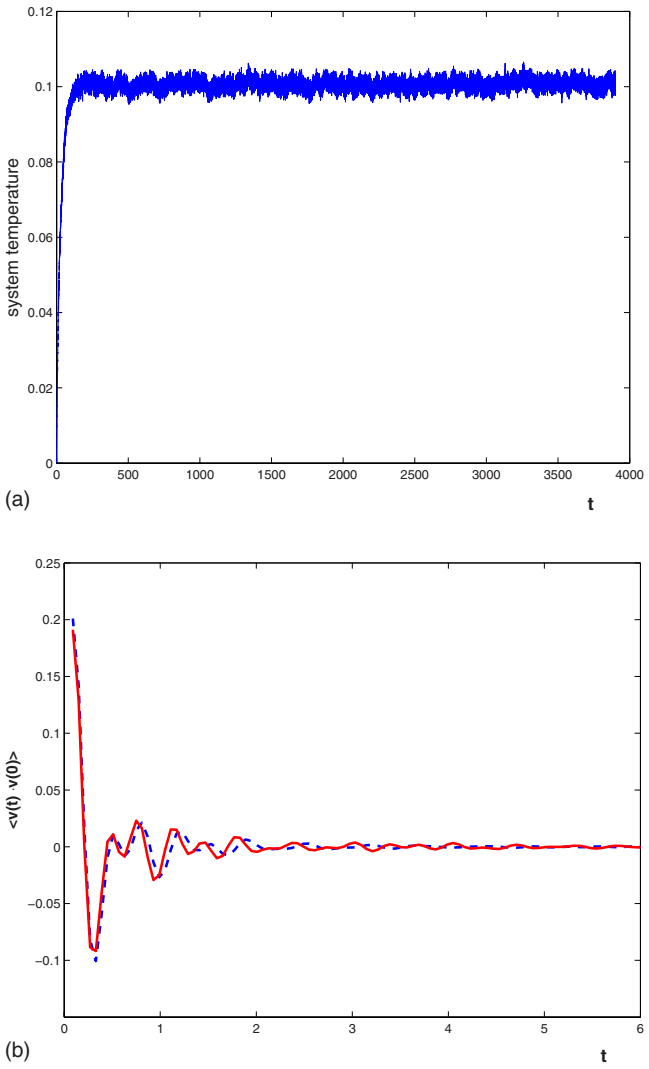

FIG. 10. (Color online) Molecular dynamics simulation in the two-dimensional Lennard-Jones system with variational boundary conditions applied at the top and bottom boundaries: (a) system temperature and (b) velocity correlation. Solid line: Velocity correlation computed from a separate microcanonical MD simulation with the same temperature. Dashed line: Velocity correlation computed from the MD simulation with finite temperature VBC applied.

$$\boldsymbol{\theta}_i = \int_t^{+\infty} D_{(-\sqrt{3}/2,1/2)}\boldsymbol{\alpha}_{i-1/2}(s) + D_{(-\sqrt{3}/2,-1/2)}\boldsymbol{\alpha}_{i+1/2}(s)ds,$$

assuming $\boldsymbol{\alpha}_{N+1/2}=\boldsymbol{\alpha}_{-N-1/2}=0$.

To test the VBCs, we consider a system with 20×20 atomic units. The system is initially at rest and is then integrated for 130 000 steps with step size $\Delta t=0.03$. Again, reduced units are used for the mass, energy, and length scales, which subsequently determine the time scale. The phase diagram of this two-dimensional lattice is quite complicated. For instance, around $k_BT=0.5$ the system develops a new structure that involves dislocations. Our applied temperature (which enters as a parameter in the VBC) is chosen to be well below this value: $k_BT=0.1$. In the first test, we monitor the system temperature, and this is plotted in Fig. 10(a). In the second test, we compute the velocity autocorrelation function after the system is equilibrated. The results are shown in Fig. 10(b) together with the exact velocity autocorrelation function computed from a separate microcanonical MD as was done in the previous example. The two results agree quite well for short times but deviate slightly at larger times. For this simulation, we have chosen $N=5$ and $M=20$ in the VBC.

C. Model of bcc iron

Next, we consider a more realistic example, a model of α-iron, a three-dimensional bcc system. Here we will use physical units. The atomic potential used is the embedded atom potential developed in Ref. 45. The system studied is a three-dimensional rectangular sample, with the three orthogonal axes along the [110], [1$\bar{1}$0], and [001] directions, respectively. The system has the dimension of $16\times 16\times 6$ atom units. VBC with temperature $k_BT=400$ K is applied to the left and right boundaries. Along the other two directions, periodic boundary conditions are applied. In the VBC, we choose the spatial stencil to consist of 25 atoms, with 5 atoms in each tangential direction, and we set $M=20$. In the simulation, we set the time step to $\Delta t=0.0246$ ps. The system is initially at rest and is then integrated for 150 000 steps. Figure 11 shows the numerical results including the system temperature [Fig. 11(a)] and the velocity autocorrelation [Fig. 11(b)]. After about 30 000 steps, the system has settled down to an equilibrium at the correct temperature. In addition, the velocity correlation function agrees quite well with the exact values.

VII. CONCLUSION

We have presented a theoretical framework for finding effective boundary conditions for molecular dynamics simulations of crystalline solids at finite temperature, and we have presented practical applications of this framework. Heat bath atoms are modeled using a Kac model. The Mori-Zwanzig formalism is used to eliminate the bath atoms and represent their effects in the form of GLEs. However, key to the success of this framework is the fact that we can go beyond the Mori-Zwanzig formalism and formulate approximate GLEs that are much more local than the exact ones. The approximate GLEs are obtained using a variational formulation of the exact GLEs.

Although there are many possibilities for improving and simplifying the technical aspects of the boundary conditions developed here, we feel that this is at least the right theoretical framework to think about the problem. It naturally embodies two limiting situations: zero temperature and static problems. The kernels are the same as the nonreflecting kernels at zero temperature. The noise is determined using the fluctuation-dissipation theorem, through which a natural connection is made with the static case in the form of the boundary conditions in the Hamiltonian. In some sense, the boundary conditions for dynamics at finite temperature are a combination of these two ingredients.

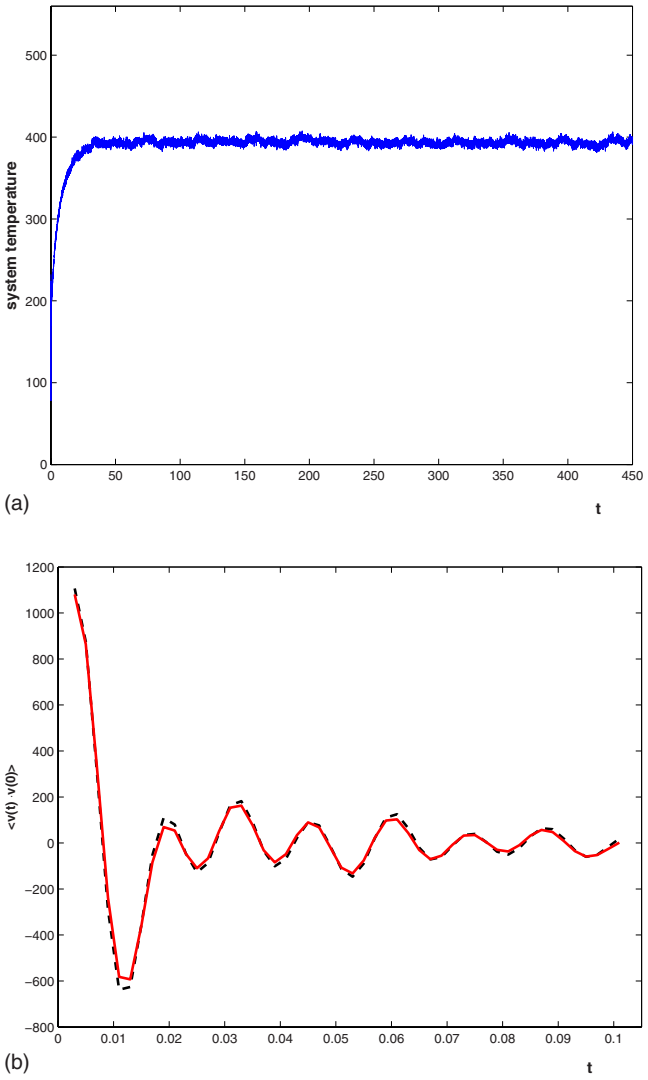

FIG. 11. (Color online) Molecular dynamics simulation of the three-dimensional bcc iron with VBC applied at the left and right boundaries: (a) system temperature and (b) velocity correlation function. Solid line: Velocity correlation computed from a separate microcanonical MD simulation with the same temperature. Dashed line: Velocity correlation function computed from the MD simulation with finite temperature VBC applied. The unit for time is 8.2 ps.

There are at least three possible applications of these boundary conditions.

(1) As a thermostat. Noise only acts on boundary atoms, not the interior atoms. This is closer to the physical situation.

(2) As a boundary condition for molecular dynamics. In particular, we can naturally extend the current framework to incorporate nontrivial external boundary conditions such as loading.

(3) As an interface condition for coupled continuum-MD modeling methods. This was the original motivation for developing such boundary conditions, and the changes required for this setting will be discussed in separate publications.

Extending the current method to fluids does not seem straightforward. Although the GLEs can, in principle, be derived and memory kernels can be obtained from test simulations as have been done in Refs. 14 and 16, the particles can move outside the system and new particles have to be introduced and inserted back to the system. Furthermore, there is no underlying lattice structure on which efficient approximations can be made.

ACKNOWLEDGMENTS

We thank Eric Vanden-Eijnden and Jerry Yang for helpful discussions. The work of W.E is supported in part by ONR Grant No. N00014-01-1-0674 and DOE Grant No. DE-FG02-03ER25587. The work of X.L. is supported in part by NSF Grant No. DMS-0609610.

APPENDIX A: DERIVATION OF THE GENERALIZED LANGEVIN EQUATION

For completeness, we provide the details for the derivation of the GLE. Fix i such that $\mathbf{r}_i \cdot \mathbf{n} > 0$. We first pick $\varphi = \mathbf{u}_i$. In this case, notice that

$$P\mathbf{v}_j = \mathbf{v}_j. \tag{A1}$$

Therefore, $L\varphi(0) = \mathbf{v}_i(0)$, $PL\varphi(0) = \mathbf{v}_i(0)$, and $QL\varphi(0) = 0$. Therefore, the equation is unchanged after the projection procedure

$$\dot{\mathbf{u}}_i = \mathbf{v}_i.$$

Now, we let $\varphi = m\mathbf{v}_i$ for $\mathbf{v}_i \cdot \mathbf{n} > 0$. Next, we will explicitly compute the projection operators P and Q. For this purpose, we first arrange the lattice points in such a way that $(\mathbf{r}_i - \mathbf{r}_j) \cdot \mathbf{n} > 0$ if $i < j$. This way of indexing the atoms implies that in the reference coordinate, for any atom i, all the atoms with larger indices are on its right. The second step to simplify the calculation is to rewrite quadratic terms in the Hamiltonian (10) as

$$\frac{1}{2}\sum_i \sum_k \mathbf{u}_i^T D_k \mathbf{u}_{i+k} = \frac{1}{2}\sum_i \left(\mathbf{u}_i - \sum_{k\in K} B_k \mathbf{u}_{i+k}\right)^T \times A\left(\mathbf{u}_i - \sum_{k\in K} B_k \mathbf{u}_{i+k}\right). \tag{A2}$$

Here, the set K is of the form $\{k > 0, |\mathbf{r}_k| \leq r_c\}$ with some cut-off distance r_c that should be provided by the atomic potential V. For convenience, it will be assumed that for any atom i, the set $\{\mathbf{r}_{i+k}, k \in K\}$ consists of all the atoms within the cut-off radius with higher indices. By matching the force constants, one finds that the matrices A and B_k are related to the force constants by

$$A + \sum_{j\in K} B_j^T A B_j = D_0, \quad -AB_k + \sum_{\substack{j\in K \\ j+k\in K}} B_j^T A B_{j+k} = D_k. \tag{A3}$$

The identity in Eq. (A2) needs to be corrected at the interface since it produces excessive cross terms for the retained variables. Because the interaction between the re-

tained variables is already included in the function V, this term must be removed, resulting in

$$H = V(\hat{\mathbf{u}}) + \frac{1}{2}\sum_i m\mathbf{v}_i^2 + \frac{1}{2}\sum_{\mathbf{r}_i\cdot\mathbf{n}\leqslant 0}\left(\mathbf{u}_i - \sum_{k\in K} B_k\mathbf{u}_{i+k}\right)^T A\left(\mathbf{u}_i - \sum_{k\in K} B_k\mathbf{u}_{i+k}\right) - \sum_{\substack{\mathbf{r}_i\cdot\mathbf{n}>0\\ \mathbf{r}_j\cdot\mathbf{n}>0}}\ \sum_{\substack{k\in K\\ \mathbf{r}_{i-k}\cdot\mathbf{n}\leqslant 0\\ \mathbf{r}_{j-k}\cdot\mathbf{n}\leqslant 0}} \frac{1}{2}\mathbf{u}_i^T B_k^T A B_{j-i+k}\mathbf{u}_j + \sum_{\mathbf{r}_i\cdot\mathbf{n}\leqslant 0}\ \sum_{\substack{k\in K\\ \mathbf{r}_{i-k}\cdot\mathbf{n}\leqslant 0}} \frac{1}{2}\mathbf{u}_i^T D_{-k}\mathbf{u}_i. \tag{A4}$$

This representation of the quadratic terms is motivated by the previous example for independent harmonic oscillators, and it greatly simplifies the calculation. In particular, let

$$\boldsymbol{\xi}_j = A^{1/2}[\mathbf{u}_j(0) - \sum_{k\in K} B_k\mathbf{u}_{j+k}(0)], \tag{A5}$$

which is a discrete analog of strain gradient, and we have for $\mathbf{r}_j\cdot\mathbf{n}\leqslant 0$

$$P\boldsymbol{\xi}_j = 0, \quad Q\boldsymbol{\xi}_j = \boldsymbol{\xi}_j.$$

To compute the first term in Eq. (8), we have for $\mathbf{r}_i\cdot\mathbf{n}>0$

$$L\mathbf{v}_i(0) = -\nabla_{\mathbf{u}_i}V(\hat{\mathbf{u}}(0)) + \sum_{\substack{k\in K\\ \mathbf{r}_{i-k}\cdot\mathbf{n}\leqslant 0}} B_k^T A^{1/2}\boldsymbol{\xi}_{i-k} - \sum_{\substack{k\in K\\ \mathbf{r}_{i-k}\cdot\mathbf{n}\leqslant 0\\ \mathbf{r}_{j-k}\cdot\mathbf{n}\leqslant 0}} B_k^T A B_{j-i+k}\mathbf{u}_j(0) - \sum_{\substack{k\in K\\ \mathbf{r}_{i-k}\cdot\mathbf{n}\leqslant 0}} D_{-k}\mathbf{u}_i(0).$$

Therefore, we get

$$PL\mathbf{v}_i = -\nabla_{\mathbf{u}_i}V(\hat{\mathbf{u}}(0)) + \sum_{\substack{k\in K\\ \mathbf{r}_{i-k}\cdot\mathbf{n}\leqslant 0\\ \mathbf{r}_{j-k}\cdot\mathbf{n}\leqslant 0}} B_k^T A B_{j-i+k}\mathbf{u}_j(0) - \sum_{\substack{k\in K\\ \mathbf{r}_{i-k}\cdot\mathbf{n}\leqslant 0}} D_{-k}\mathbf{u}_i(0).$$

More generally, we have the following lemma.

Lemma A.1. The first term in the GLE (8) becomes

$$e^{tL}PL\mathbf{v}_i(0) = -\nabla_{\mathbf{u}_i}V(\hat{\mathbf{u}}(t)) + \sum_{\substack{k\in K\\ \mathbf{r}_{i-k}\cdot\mathbf{n}\leqslant 0\\ \mathbf{r}_{j-k}\cdot\mathbf{n}\leqslant 0}} B_k^T A B_{j-i+k}\mathbf{u}_j - \sum_{\substack{k\in K\\ \mathbf{r}_{i-k}\cdot\mathbf{n}\leqslant 0}} D_{-k}\mathbf{u}_i. \tag{A6}$$

Applying the operator QL, we have

$$QL\mathbf{v}_i(0) = \sum_{\substack{k\in K\\ \mathbf{r}_{i-k}\cdot\mathbf{n}\leqslant 0}} B_k^T A^{1/2}\boldsymbol{\xi}_{i-k} = \sum_{\substack{\mathbf{r}_j\cdot\mathbf{n}\leqslant 0\\ i-j\in K}} B_{i-j}^T A^{1/2}\boldsymbol{\xi}_j. \tag{A7}$$

Next, we compute the random force term $F_i(t)$. The orthogonality condition $PF_i=0$ suggests that we seek $F_i(t)$ with the following form:

$$F_i(t) = \sum_{\mathbf{r}_j\cdot\mathbf{n}\leqslant 0} C_{i,j}(t)\boldsymbol{\xi}_j + S_{i,j}(t)\mathbf{v}_j(0), \tag{A8}$$

with $S_{i,j}(t)$ and $C_{i,j}(t)$ to be determined. This form of representing the random force can be validated by expanding the operator e^{tQL} in power series in the equation

$$F_i(t) = e^{tQL}QL\mathbf{v}_i(0).$$

For each term in the expansion, the operator QL is applied repeatedly: The operator Q will confine the summation to the atoms on the left, and thus the operator L will always produce linear terms.

Now, notice that F_i solves the equation

$$\dot{F}_i = QLF_i.$$

Substituting Eq. (A8) into the above equation, we have

$$QLF_i(t) = \sum_j [C_{i,j}(t)A^{1/2} - \sum_{k\in K} C_{i,j-k}A^{1/2}B_k]\mathbf{v}_j(0) + \sum_j [-S_{i,j}(t)A^{1/2} + \sum_{k\in K} S_{i,j+k}B_k^T A^{1/2}]\boldsymbol{\xi}_j/m. \tag{A9}$$

Consequently, for any $\mathbf{r}_j\cdot\mathbf{n}\leqslant 0$, we have the following system of equations:

$$m\dot{C}_{i,j} = -S_{i,j}A^{1/2} + \sum_k S_{i,j+k}B_k^T A^{1/2},$$

$$\dot{S}_{i,j} = C_{i,j}A^{1/2} - \sum_k C_{i,j-k}A^{1/2}B_k,$$

$$S_{i,j}(0) = 0, \tag{A10}$$

$$C_{i,j}(t) = 0 \quad \text{for } i-j\notin K,$$

$$C_{i,j}(0) = B_{i-j}^T A^{1/2} \quad \text{for } i-j\in K.$$

Lemma A.2. $F_i(t)$ is a stationary Gaussian process, and for $i-j\in K$, we have

$$\langle F_i(t)F_j(0)^T\rangle = k_BT\sum_{\mathbf{r}_k\cdot\mathbf{n}\leqslant 0} C_{i,k}(t)A^{1/2}B_{j-k}. \tag{A11}$$

Proof. It is easy to see that $F_i(t)$ is a Gaussian process with mean zero. Notice that $\langle\boldsymbol{\xi}_i\boldsymbol{\xi}_j^T\rangle = k_BT\delta_{ij}I$. From Eq. (A8), the time correlation is given by

$$\boldsymbol{\theta}_{ij}(t,t_0) = \langle F_i(t+t_0)F_j(t_0)^T\rangle = k_BT\sum_k S_{i,k}(t+t_0)S_{j,k}(t_0)^T + C_{i,k}(t+t_0)C_{j,k}(t_0)^T. \tag{A12}$$

Next, we take the time derivative of $\boldsymbol{\theta}_{ij}$ using Eqs. (A10) and (A3). With the boundary condition

$$C_{i,j} = 0 \quad \text{for } i - j \notin K,$$

one finds that

$$\frac{d}{dt_0}\boldsymbol{\theta}_{ij}(t,t_0) = 0,$$

which proves the stationarity.

Finally, since $F_i(0) = QL\mathbf{v}_i(0)$, the time correlation can be computed by combining Eqs. (A8) and (A7). □

It remains to calculate the memory term.

Lemma A.3. The memory term in the GLE 8 takes the form

$$-\int_0^t \sum_{\mathbf{r}_j\cdot\mathbf{n}>0} \sum_{\substack{k\in K \\ \mathbf{r}_{j-k}\cdot\mathbf{n}\leqslant 0}} C_{i,j-k}(t-s)A^{1/2}B_k\mathbf{v}_j(s)ds.$$

Proof. In computing Eq. (A9), we projected out all the velocity terms for the retained variables. These terms appear in $K(t)$:

$$K(t) = PLF_i(t) = -\sum_{\mathbf{r}_j\cdot\mathbf{n}>0} \sum_{\substack{k\in K \\ \mathbf{r}_{j-k}\cdot\mathbf{n}\leqslant 0}} C_{i,j-k}(t)A^{1/2}B_k\mathbf{v}_j(0).$$

Therefore, the memory term becomes

$$\int_0^t e^{(t-s)L}K(s)ds = -\int_0^t \sum_{\mathbf{r}_j\cdot\mathbf{n}>0} \sum_{\substack{k\in K \\ \mathbf{r}_{j-k}\cdot\mathbf{n}\leqslant 0}} C_{i,j-k}(t-s)A^{1/2}B_k\mathbf{v}_j(s)ds.$$

□

Now, for $\mathbf{r}_i\cdot\mathbf{n}>0$ and $\mathbf{r}_j\cdot\mathbf{n}>0$, define

$$\boldsymbol{\theta}_{i,j}(t) = \sum_{\substack{k\in K \\ \mathbf{r}_{j-k}\cdot\mathbf{n}\leqslant 0}} C_{i,j-k}(t)A^{1/2}B_k. \tag{A13}$$

In particular, we have

$$\boldsymbol{\theta}_{i,j}(0) = \sum_{\substack{k\in K \\ \mathbf{r}_{j-k}\cdot\mathbf{n}\leqslant 0}} B_k^T A B_{j-i+k}.$$

Collecting all the three terms, we have the following theorem.

Theorem A.1. For the retained variables, the following GLEs hold:

$$m\ddot{\mathbf{u}}_i = -\nabla_{\mathbf{u}_i}V - \left(\sum_{\substack{k\in K \\ \mathbf{r}_{i-k}\cdot\mathbf{n}\leqslant 0}} D_{-k}\right)\mathbf{u}_i + \sum_{\mathbf{r}_j\cdot\mathbf{n}>0}\left[\boldsymbol{\theta}_{i,j}(0)\mathbf{u}_j(t) - \int_0^t \boldsymbol{\theta}_{i,j}(s)\dot{\mathbf{u}}_j(t-s)ds\right] + F_i(t). \tag{A14}$$

Provided that the initial statistics is given by the Gibbs distribution, the random processes $F_i(t)$ are stationary Gaussian processes. In addition, the second fluctuation-dissipation theorem holds

$$\langle F_i(t)F_j(0)^T\rangle = k_BT\boldsymbol{\theta}_{i,j}(t). \tag{A15}$$

In the GLE (11), both the memory term and random noise term are expressed in terms of the functions $S_{i,j}$ and $C_{i,j}$. To find these functions, take the time derivative of the second equation in Eq. (10) and combine it with the first equation. One then finds

$$\begin{aligned} m\ddot{S}_{i,j}^T &= A\left(-S_{i,j}^T + \sum_{k\in K} B_k S_{i,j+k}^T\right) \\ &\quad + \sum_{k\in K} B_k^T A\left(-S_{i,j-k}^T + \sum_{k'\in K} B_k S_{i,j-k+k'}^T\right) \\ &= -\sum_k D_k S_{i,j+k}^T, \end{aligned} \tag{A16}$$

where Eq. (A3) has been used. This shows that each row of the matrix $S_{i,j}$ obeys the linearized Newton's equation of motion. Meanwhile, the initial condition is given by

$$S_{i,j}(0) = 0, \quad \dot{S}_{i,j}(0) = C_{i,j}(0)A^{1/2} - \sum_k C_{i,j-k}(0)A^{1/2}B_k.$$

Hence, in principle, the memory kernels can be computed by solving Eq. (A16), which in turn determines the random force term. This calculation also indicates that the memory kernels, which are only related to the functions $S_{i,j}(t)$ and $C_{i,j}(t)$, are temperature independent. This is a result of the harmonic approximation beyond which the kernels can be dependent on the temperature.[46] Finally, the memory kernels are related to the lattice Green's functions. More discussion can be found in Ref. 18.

APPENDIX B: TWO FORMS OF THE BOUNDARY CONDITION

The GLEs derived in the previous section only involve the atoms in the computational domain. They seem to differ from typical form of boundary conditions for MD which asks for the displacement of the outside atoms that are adjacent to the boundary. The following calculation shows that the GLEs can be recast into that form.

Proposition B.1. Let $\alpha_{ij}(t)$ and $G_i(t)$ be functions so that

$$\sum_{\substack{k\in K \\ \mathbf{r}_{i-k}\cdot\mathbf{n}\leqslant 0}} D_{-k}\int_t^\infty \boldsymbol{\alpha}_{i-k,j}(s)ds = \boldsymbol{\theta}_{i,j}(t), \qquad \sum_{\substack{k\in K \\ \mathbf{r}_{i-k}\cdot\mathbf{n}\leqslant 0}} D_{-k}G_{i-k} = F_i. \tag{B1}$$

Then, the GLEs (11) are equivalent to

$$m\ddot{\mathbf{u}}_i = -\nabla_{\mathbf{u}_i}H \quad \text{for } \mathbf{r}_i\cdot\mathbf{n} > 0, \tag{B2}$$

with the following boundary condition for the heat bath variables $\mathbf{v}_i\cdot\mathbf{n}\leqslant 0$:

$$\mathbf{u}_i(t) = \sum_{\mathbf{r}_j\cdot\mathbf{n}>0} \int_t^\infty \boldsymbol{\alpha}_{i,j}(s)ds\mathbf{u}_j(0) + \int_0^t \boldsymbol{\alpha}_{i,j}(s)\mathbf{u}_j(t-s)ds + G_i(t). \tag{B3}$$

Proof. For the atoms associated with the retained variable $\mathbf{n}_i$, the force due to the heat bath variables is

$$\mathbf{f}_i^{ex} = \sum_{\substack{k\in K \\ \mathbf{r}_{i-k}\cdot\mathbf{n}\leqslant 0}} D_{-k}(\mathbf{u}_{i-k} - \mathbf{u}_i).$$

With the boundary condition (B3) applied, we have

$$\mathbf{f}_i^{ex} = -\sum_{\substack{k\in K \\ \mathbf{r}_{i-k}\cdot\mathbf{n}\leqslant 0}} D_{-k}\mathbf{u}_i + \sum_{\substack{k\in K \\ \mathbf{r}_{i-k}\cdot\mathbf{n}\leqslant 0}} D_{-k} \sum_{\mathbf{r}_j\cdot\mathbf{n}>0} \int_t^\infty \boldsymbol{\alpha}_{i-k,j}(s)ds\mathbf{u}_j(0) + \int_0^t \boldsymbol{\alpha}_{i-k,j}(s)\mathbf{u}_j(t-s)ds + \sum_{\substack{k\in K \\ \mathbf{r}_{i-k}\cdot\mathbf{n}\leqslant 0}} D_{-k}G_{i-k}.$$

Substituting this into Eq. (B2) for the ith atom and using the identities in Eq. (B1), we arrive at the GLEs (11). □

Because the atomic interaction is usually of finite range, the boundary condition (B3) is only necessary for those outside atoms such that $\mathbf{r}_{i+k}\cdot\mathbf{n}>0$ for some $k\in K$. Therefore, it is natural to assume that

$$\boldsymbol{\alpha}_{ij}(t) = 0 \quad \text{if } j-i \notin K.$$

At zero temperature $T=0$, we have $F_i=0$. Hence, $\boldsymbol{\xi}_i=0$ for $\mathbf{r}_i\cdot\mathbf{n}\leqslant 0$. So, we require that $G_i=0$ and in light of Eq. (A5) we require that $\mathbf{u}_i(0)=0$ for those atoms such that $\mathbf{r}_{i-k}\cdot\mathbf{n}\leqslant 0$ for some $k\in K$. Therefore, at zero temperature the first term and the last term in Eq. (B3) should vanish, leading to

$$\mathbf{u}_i(t) = \sum_{\mathbf{r}_j\cdot\mathbf{n}>0} \int_0^t \boldsymbol{\alpha}_{i,j}(s)\mathbf{u}_j(t-s)ds. \tag{B4}$$

This is the more familiar form of the boundary condition at zero temperature.

[1] X. Li and W. E (unpublished).
[2] W. E and Z. Huang, Phys. Rev. Lett. **87**, 135501 (2001).
[3] W. E and Z. Huang, J. Comput. Phys. **182**, 234 (2002).
[4] X. Li and W. E, J. Mech. Phys. Solids **56**, 1650 (2005).
[5] X. Li and W. E, Comm. Comp. Phys. **1**, 136 (2006).
[6] R. Zwanzig, J. Chem. Phys. **32**, 1173 (1960).
[7] R. Zwanzig, in *Systems Far from Equilibrium*, edited by L. Garrido (Interscience, New York, 1980).
[8] H. Mori, Prog. Theor. Phys. **33**, 423 (1965).
[9] R. Kubo, Rep. Prog. Phys. **29**, 255 (1966).
[10] S. A. Adelman and J. D. Doll, J. Chem. Phys. **61**, 4242 (1974).
[11] S. A. Adelman and J. D. Doll, J. Chem. Phys. **64**, 2375 (1976).
[12] J. C. Tully, J. Chem. Phys. **73**, 1975 (1980).
[13] W. Cai, M. de Koning, V. V. Bulatov, and S. Yip, Phys. Rev. Lett. **85**, 3213 (2000).
[14] B. J. Berne, M. E. Tuckerman, J. E. Straub, and A. L. R. Bug, J. Chem. Phys. **93**, 5084 (1990).
[15] M. Tuckerman and B. J. Berne, J. Chem. Phys. **98**, 7301 (1993).
[16] S. Izvekov and G. A. Voth, J. Chem. Phys. **125**, 151101 (2006).
[17] G. J. Wagner, E. G. Karpov, and W. K. Liu, Comput. Methods Appl. Mech. Eng. **193**, 1579 (2004).
[18] E. G. Karpov, G. J. Wagner, and W. K. Liu, Int. J. Numer. Methods Eng. **62**, 1250 (2005).
[19] E. G. Karpov, H. S. Park, and W. K. Liu, Int. J. Numer. Methods Eng. **70**, 351 (2007).
[20] A. J. Chorin, A. Kast, and R. Kupferman, Proc. Natl. Acad. Sci. U.S.A. **96**, 4094 (1998).
[21] A. J. Chorin, A. Kast, and R. Kupferman, Commun. Pure Appl. Math. **52**, 1231 (1999).
[22] A. J. Chorin, O. H. Hald, and R. Kupferman, Proc. Natl. Acad. Sci. U.S.A. **97**, 6253 (2000).
[23] A. J. Chorin, O. H. Hald, and R. Kupferman, Physica D **166**, 239 (2002).
[24] H. C. Andersen, J. Chem. Phys. **72**, 2384 (1980).
[25] D. J. Evans and G. P. Morris, *Statistical Mechanics of Non-Equilibrium Liquids* (Academic, London, 1990).
[26] H. J. C. Berendsen, J. P. M. Postma, W. F. van Gunsteren, A. DiNola, and J. R. Haak, J. Chem. Phys. **81**, 3684 (1984).
[27] D. Frenkel and B. Smit, *Understanding Molecular Simulation: From Algorithms to Applications*, 2nd ed. (Academic, New York, 2002).
[28] R. E. Rudd and J. Q. Broughton, Phys. Rev. B **72**, 144104 (2005).
[29] R. Zwanzig, J. Stat. Phys. **9**, 215 (1973).
[30] G. W. Ford, M. Kac, and P. Mazur, J. Math. Phys. **6**, 504 (1965).
[31] E. B. Tadmor, M. Ortiz, and R. Phillips, Philos. Mag. A **73**, 1529 (1996).
[32] W. E, J. Lu, and J. Z. Yang, Phys. Rev. B **74**, 214115 (2006).
[33] B. Alpert, L. Greengard, and T. Hagstrom, J. Comput. Phys. **180**, 270 (2002).
[34] L. Greengard and V. Rokhlin, J. Comput. Phys. **73**, 325 (1987).
[35] J. Z. Yang and X. Li, Phys. Rev. B **73**, 224111 (2006).
[36] M. C. Wang and G. E. Uhlenbeck, Rev. Mod. Phys. **17**, 323 (1945).
[37] M. E. Tuckerman and B. J. Berne, J. Chem. Phys. **95**, 4389 (1991).
[38] M. B. Berkowitz, J. D. Morgan, and J. A. McCammon, J. Chem. Phys. **78**, 3256 (1983).
[39] H. Monkhorst and J. Pack, Phys. Rev. B **13**, 5188 (1976).
[40] C. Zhu, R. Byrd, and J. Nocedal, ACM Trans. Math. Softw. **23**,

550 (1997).
[41] S. Nosé, J. Chem. Phys. **81**, 511 (1984).
[42] W. G. Hoover, Phys. Rev. A **31**, 1695 (1985).
[43] M. Moseler, J. Nordiek, and H. Haberland, Phys. Rev. B **56**, 15439 (1997).
[44] S. Qu, V. Shastry, W. A. Curtin, and R. E. Miller, Modell. Simul. Mater. Sci. Eng. **13**, 1103 (2005).
[45] V. Shastry and D. Farkas, MRS Symposium Proceedings No. 409 (Materials Research Society, Pittsburgh, 1996), pp. 75–80.
[46] T. Munakata, Phys. Rev. B **33**, 8016 (1986).